Electronic Supplementary Material (ESI) for Dalton Transactions.

Supporting Information

Novel intramolecular π-π-interaction in a BODIPY system by oxidation of a single selenium center: geometrical stamping and spectroscopic and spectrometric distinctions

Youngsam Kim,[a,b] Taehong Jun,[a] Sandip V. Mulay,[b] Sudesh T. Manjare,[c] Jinseong Kwak,[d] Yunho Lee[d] and David G. Churchill[a,b*]

dchurchill@kaist.ac.kr

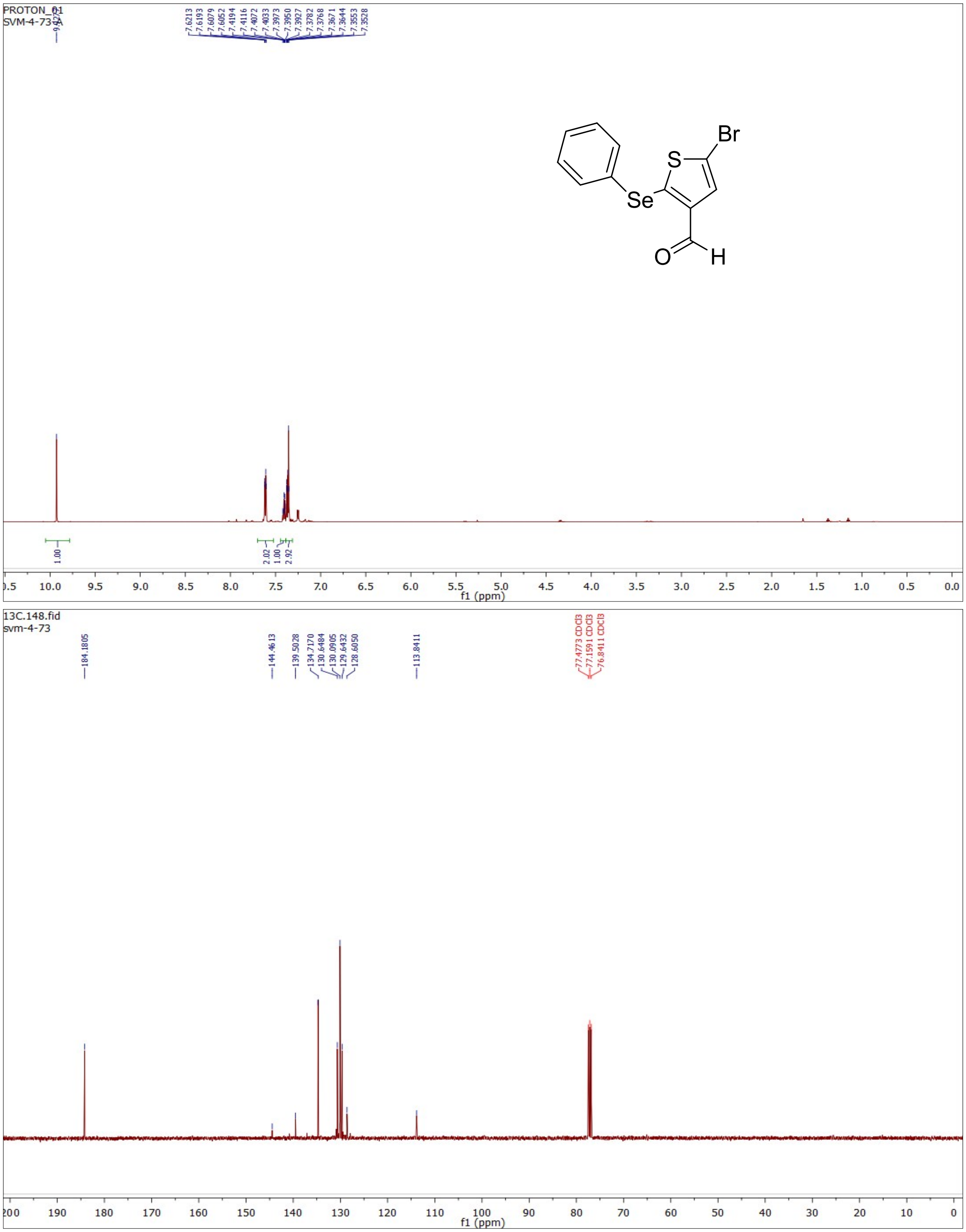

Fig. S1. (top) ^{1}H and (bottom) ^{13}C NMR spectrum of compound **2** in $CDCl_3$.

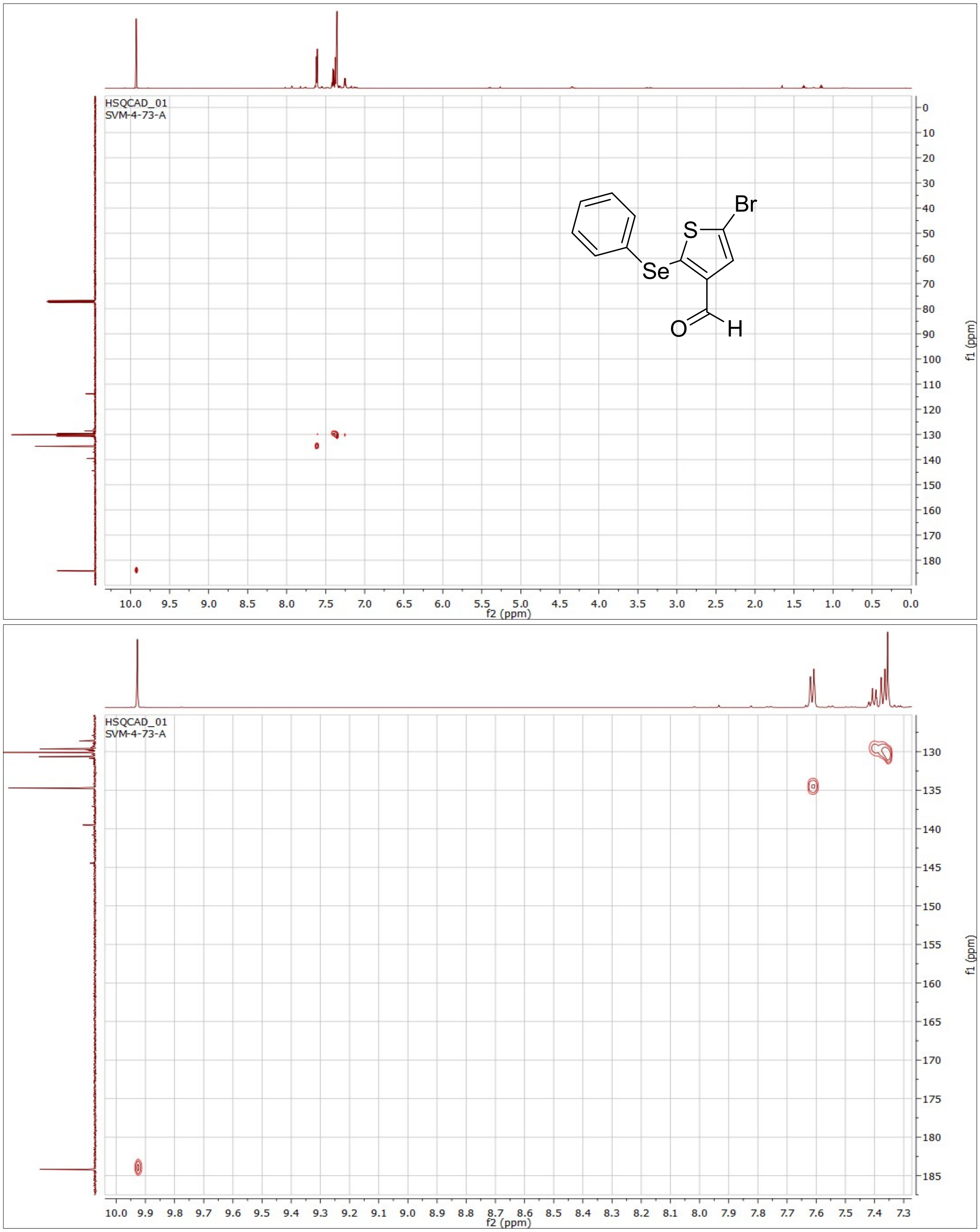

Fig. S2. (top) ^{1}H-^{13}C HSQC NMR spectrum of compound **2**, and (bottom) expanded aromatic region in $CDCl_3$.

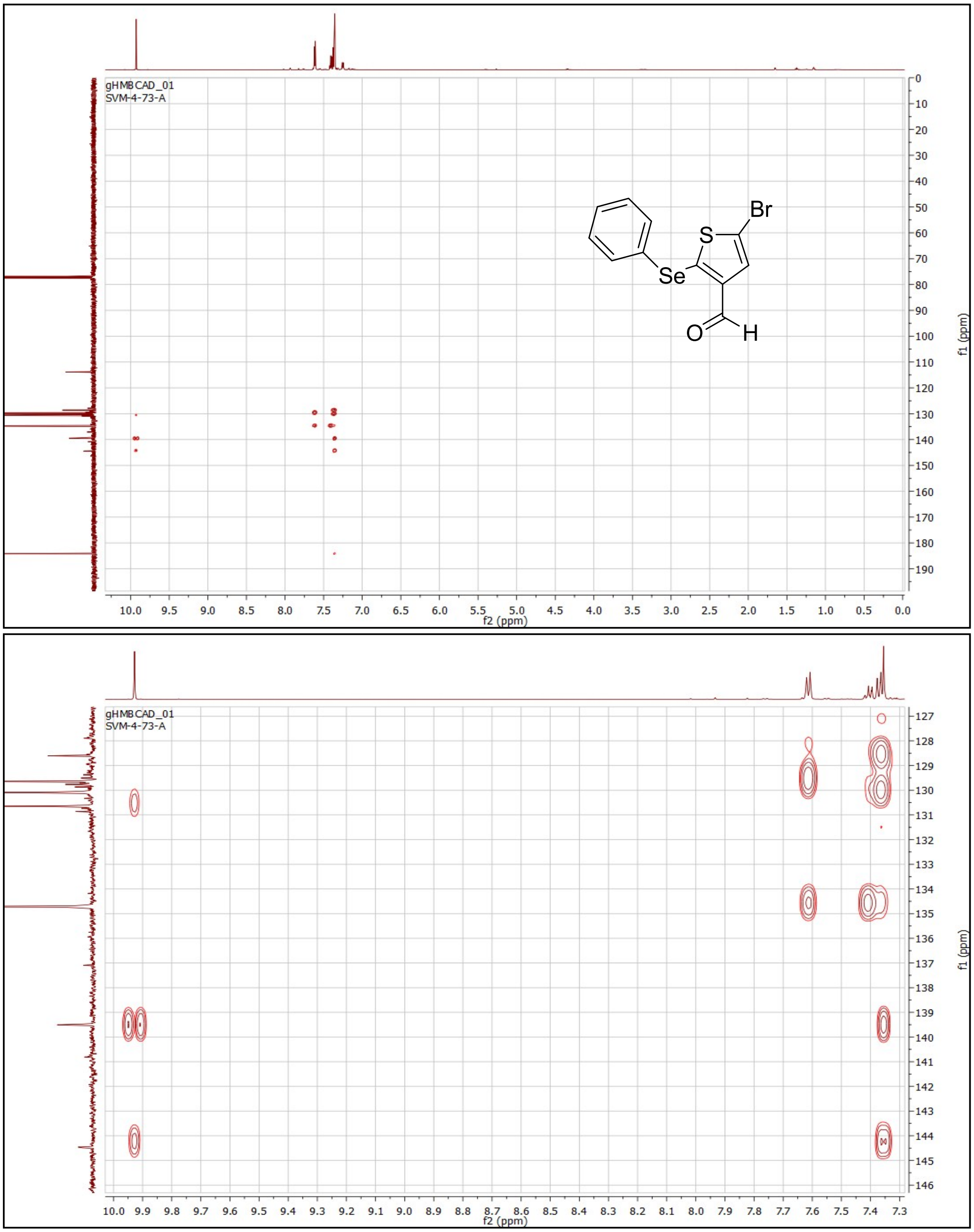

Fig. S3. (top) ^{1}H-^{13}C HMBC NMR spectrum of compound **2**, and (bottom) expanded aromatic region in $CDCl_3$.

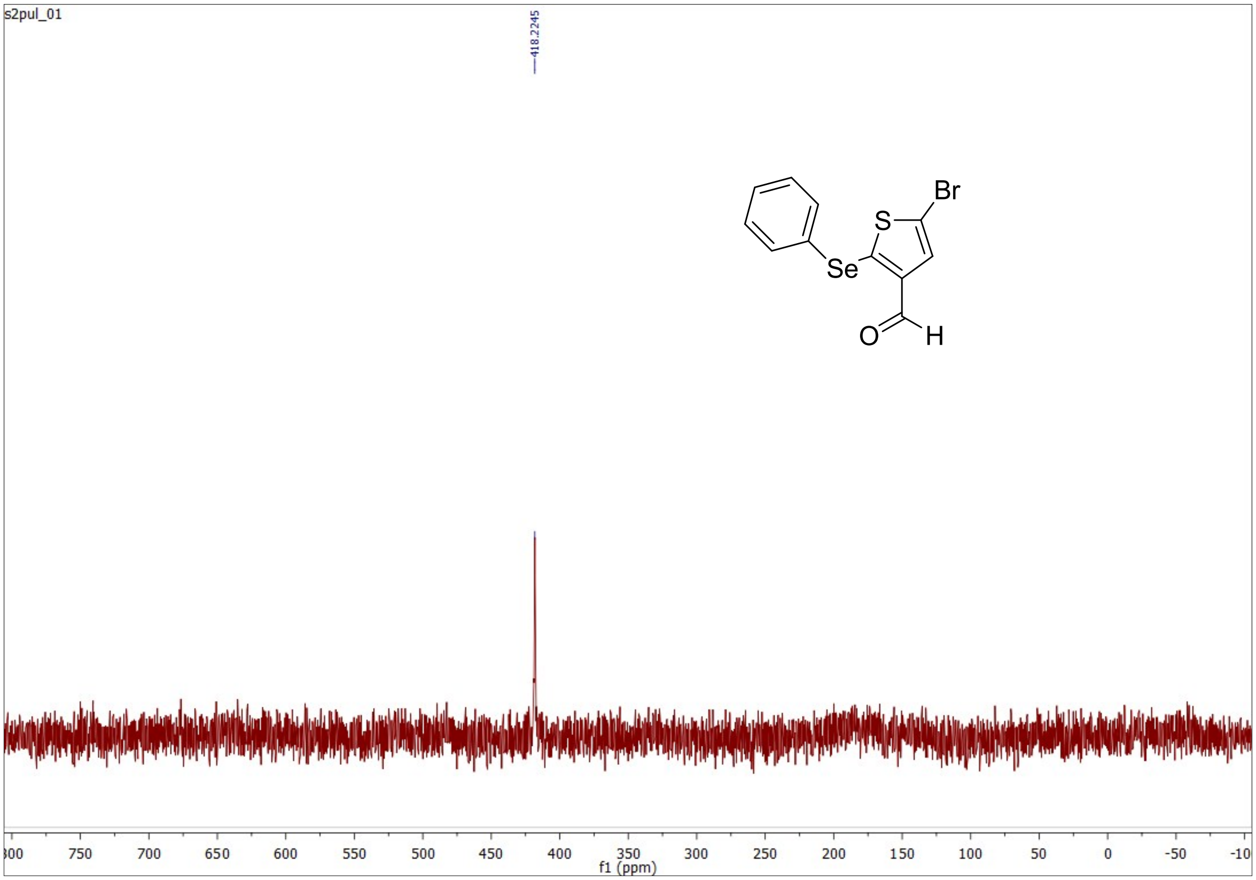

Figure S4. ^{77}Se NMR spectrum of compound **2** in CDCl$_3$.

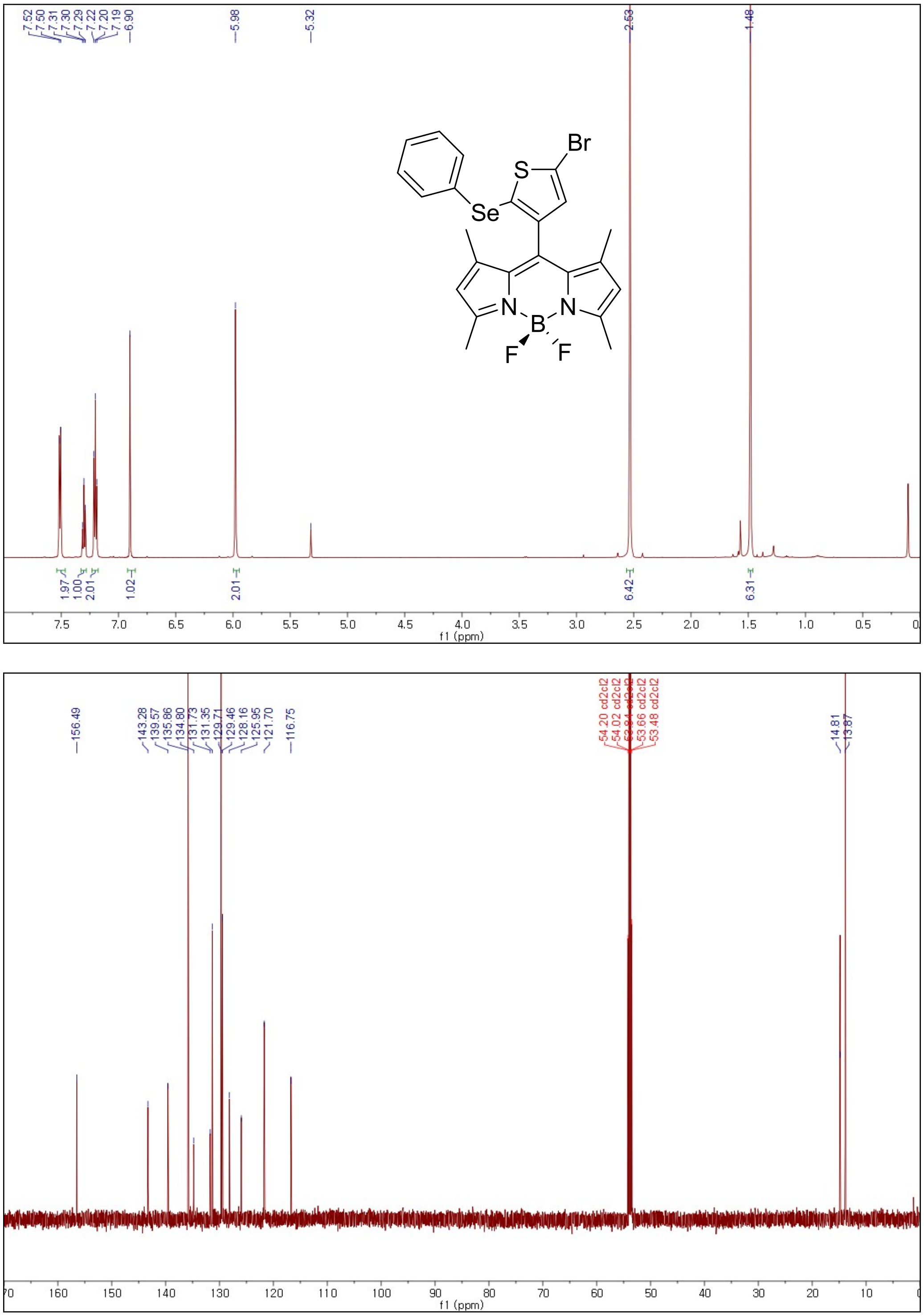

Fig. S5. (top) ^{1}H and (bottom) ^{13}C NMR spectrum of compound **3** in CD_2Cl_2.

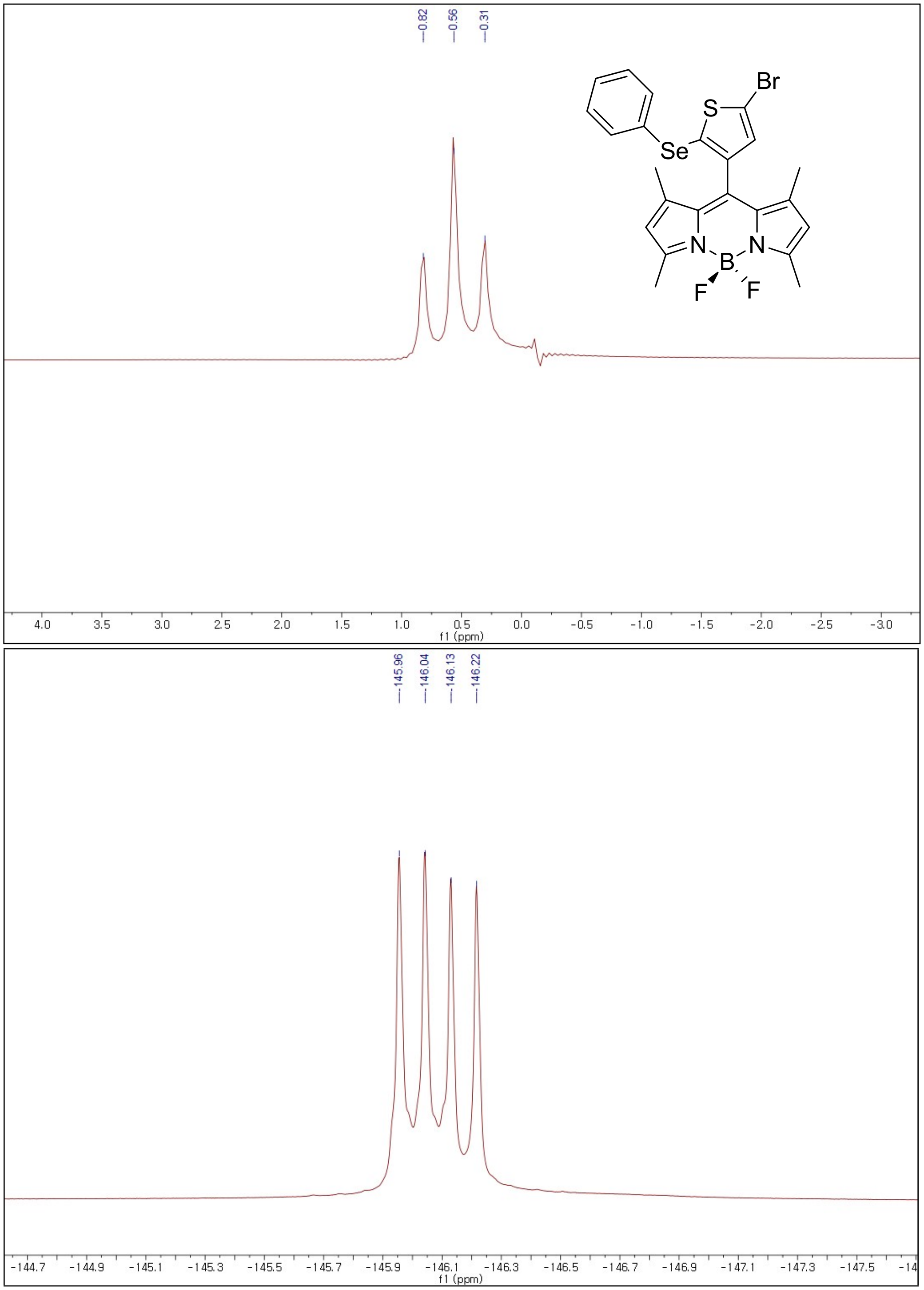

Figure S6. (top) ^{11}B and (bottom) ^{19}F NMR spectrum of compound **3** in CD_2Cl_2.

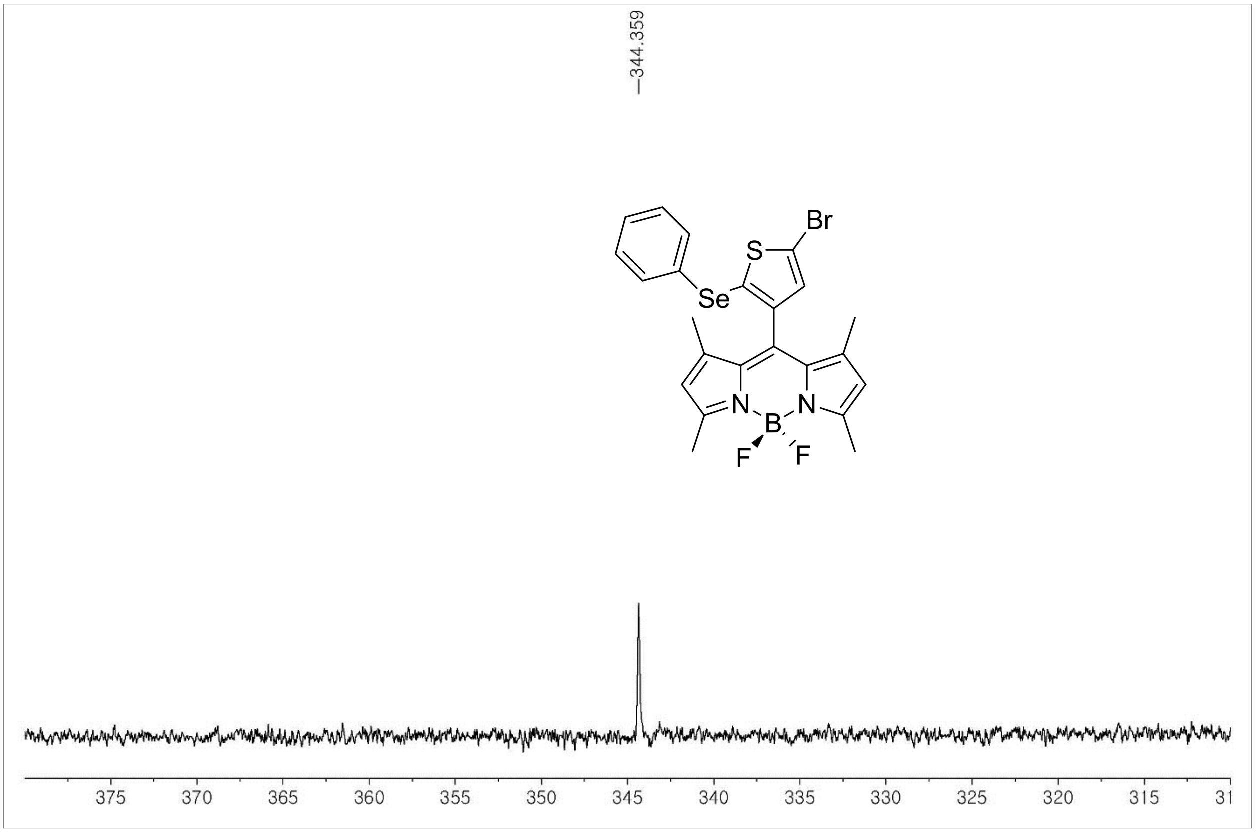

Figure S7. ^{77}Se NMR spectrum of compound **3** in CD_2Cl_2.

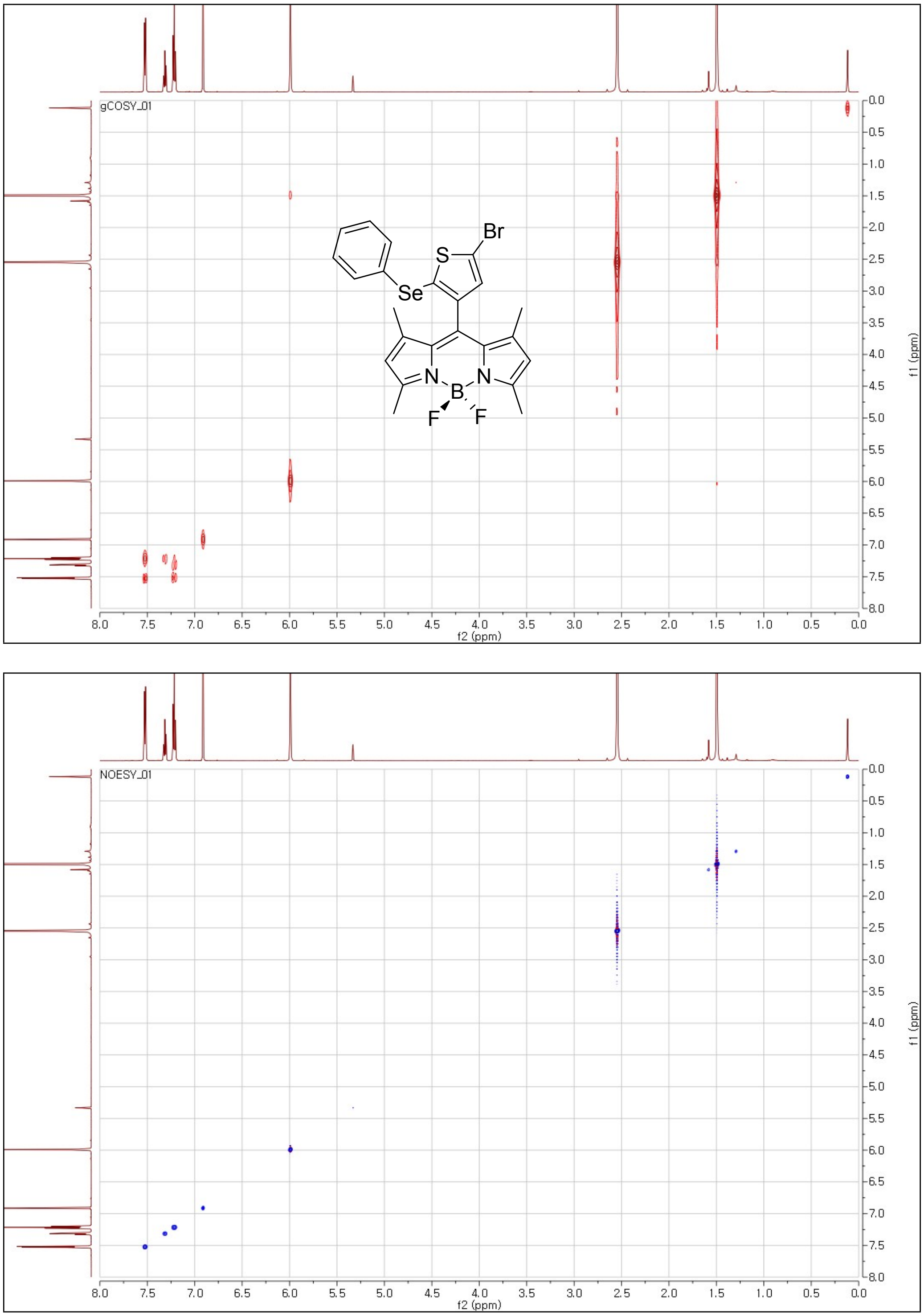

Figure S8. (top) COSY and (bottom) NOESY spectrum of compound **3** in CD_2Cl_2.

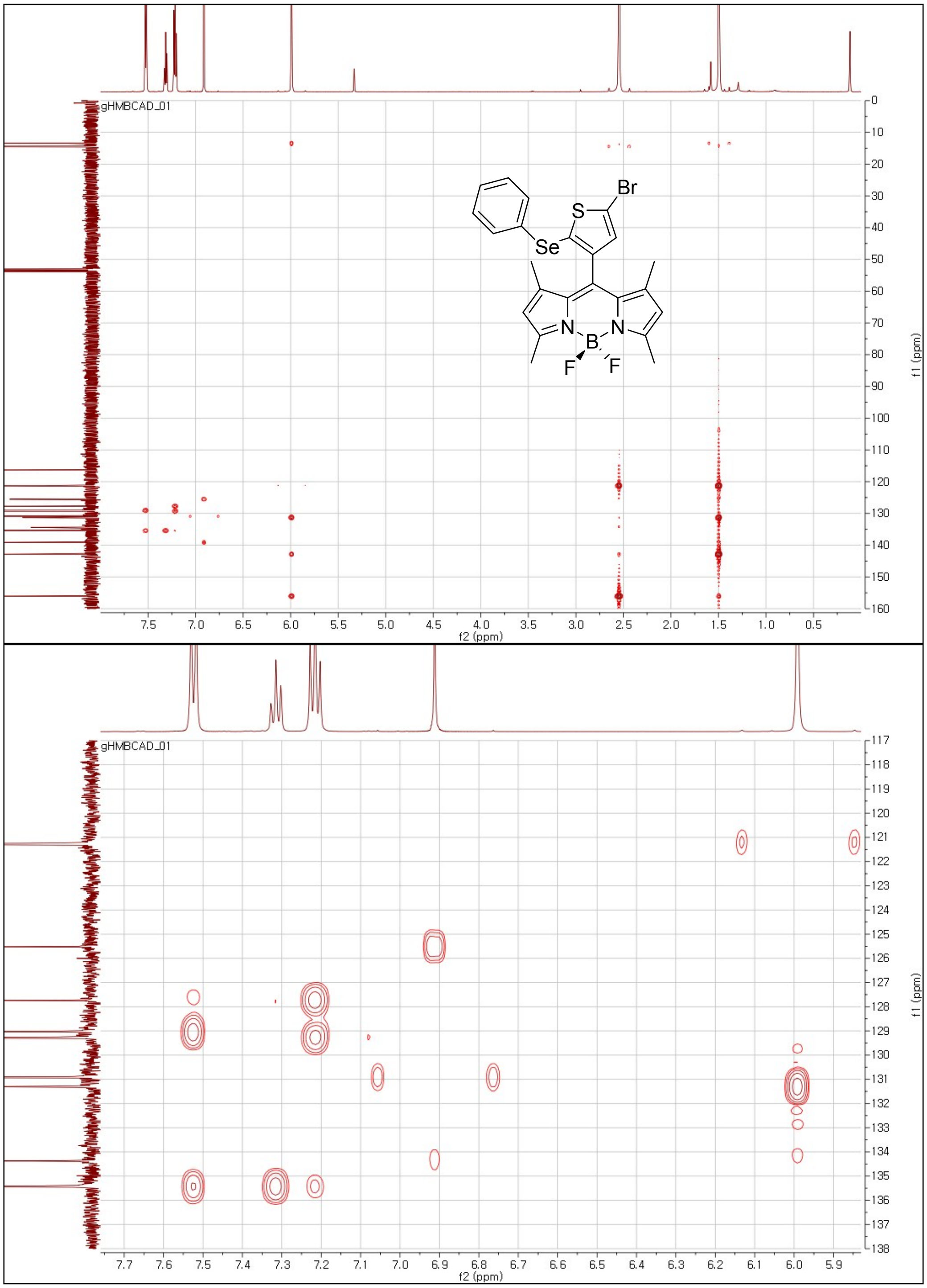

Fig. S9. (top) ^{1}H-^{13}C HMBC NMR spectrum of compound **3**, and (bottom) expanded aromatic region in CD_2Cl_2.

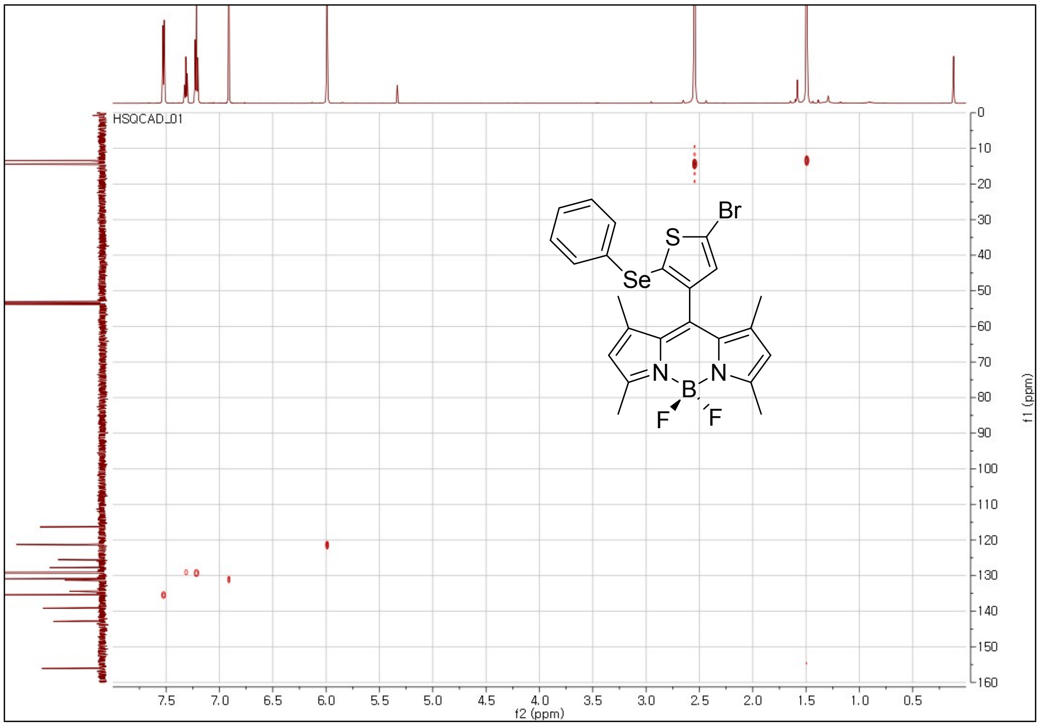

Fig. S10. (top) ^{1}H-^{13}C HSQC NMR spectrum of compound **3**, and (bottom) expanded aromatic region CD_2Cl_2.

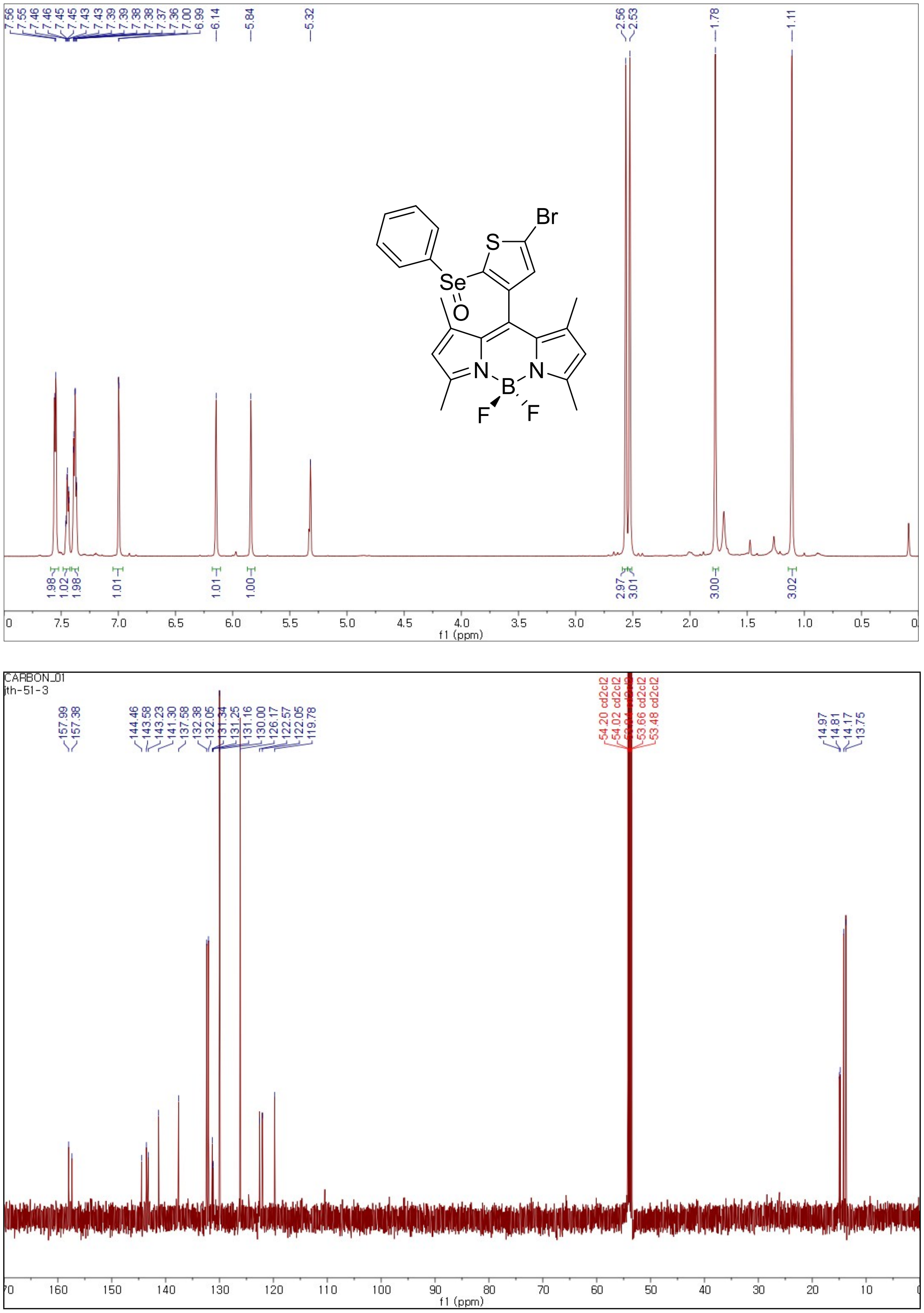

Fig. S11. (top) ^{1}H NMR and (bottom) ^{13}C NMR spectrum of compound **4** in CD_2Cl_2.

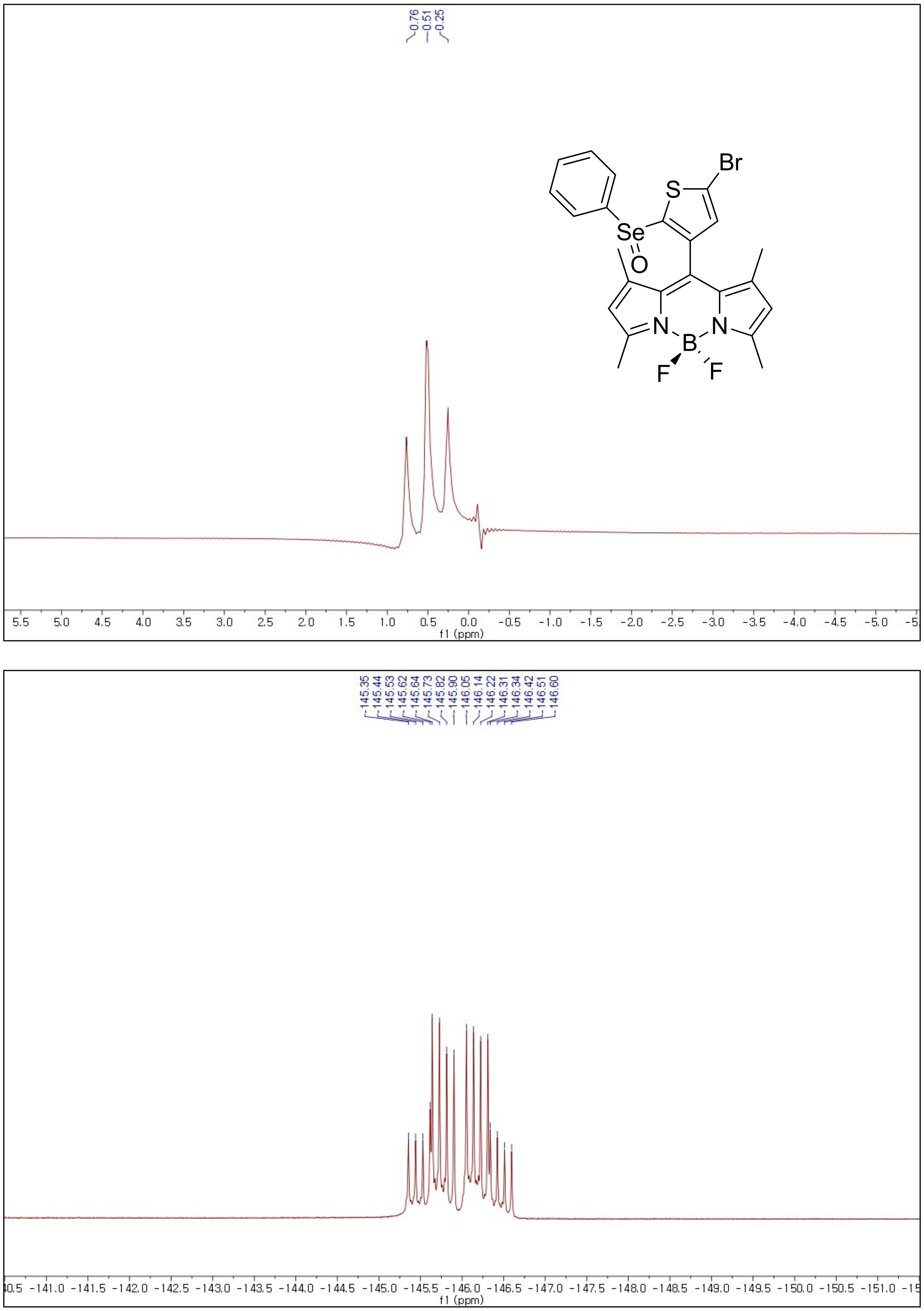

Fig. S12. (top) ^{11}B and (bottom) ^{19}F NMR spectrum of compound **4** in CD_2Cl_2.

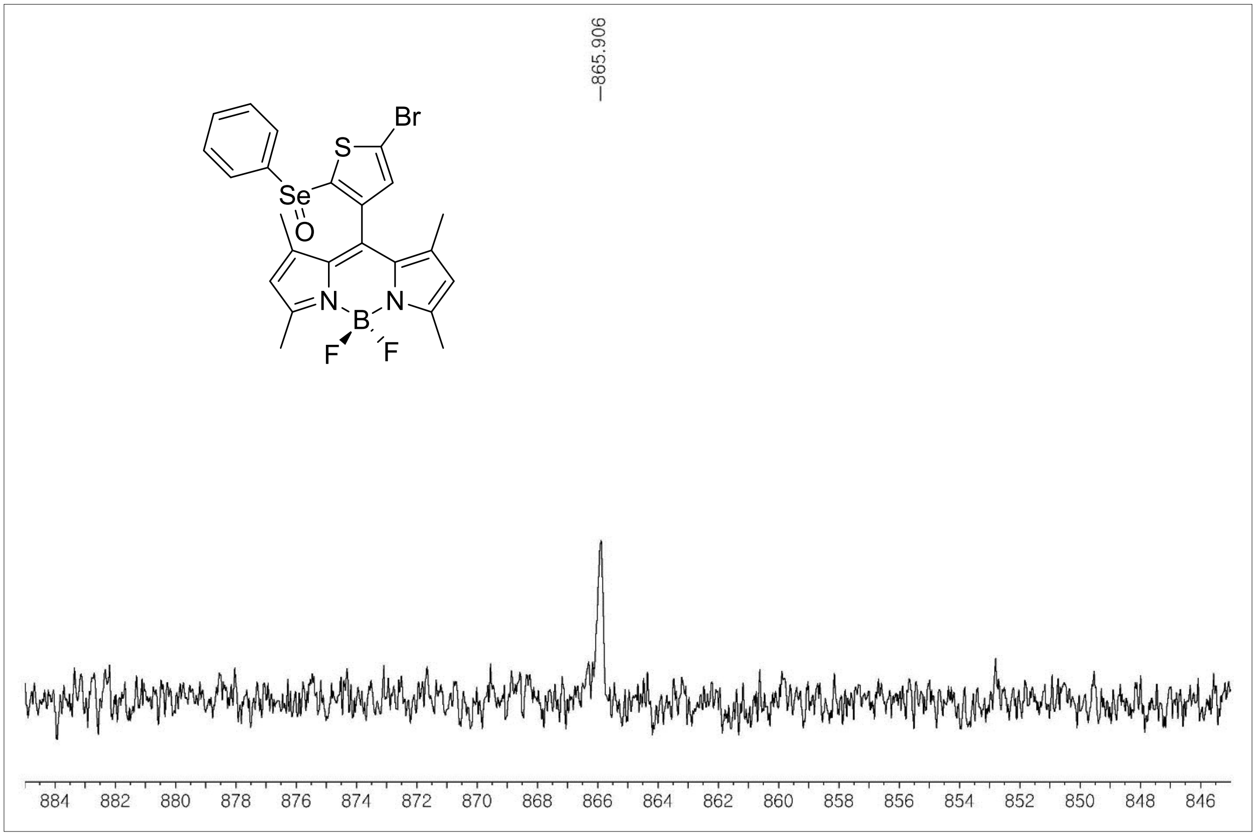

Fig. S13. ^{77}Se NMR spectrum of compound **4** in CD_2Cl_2.

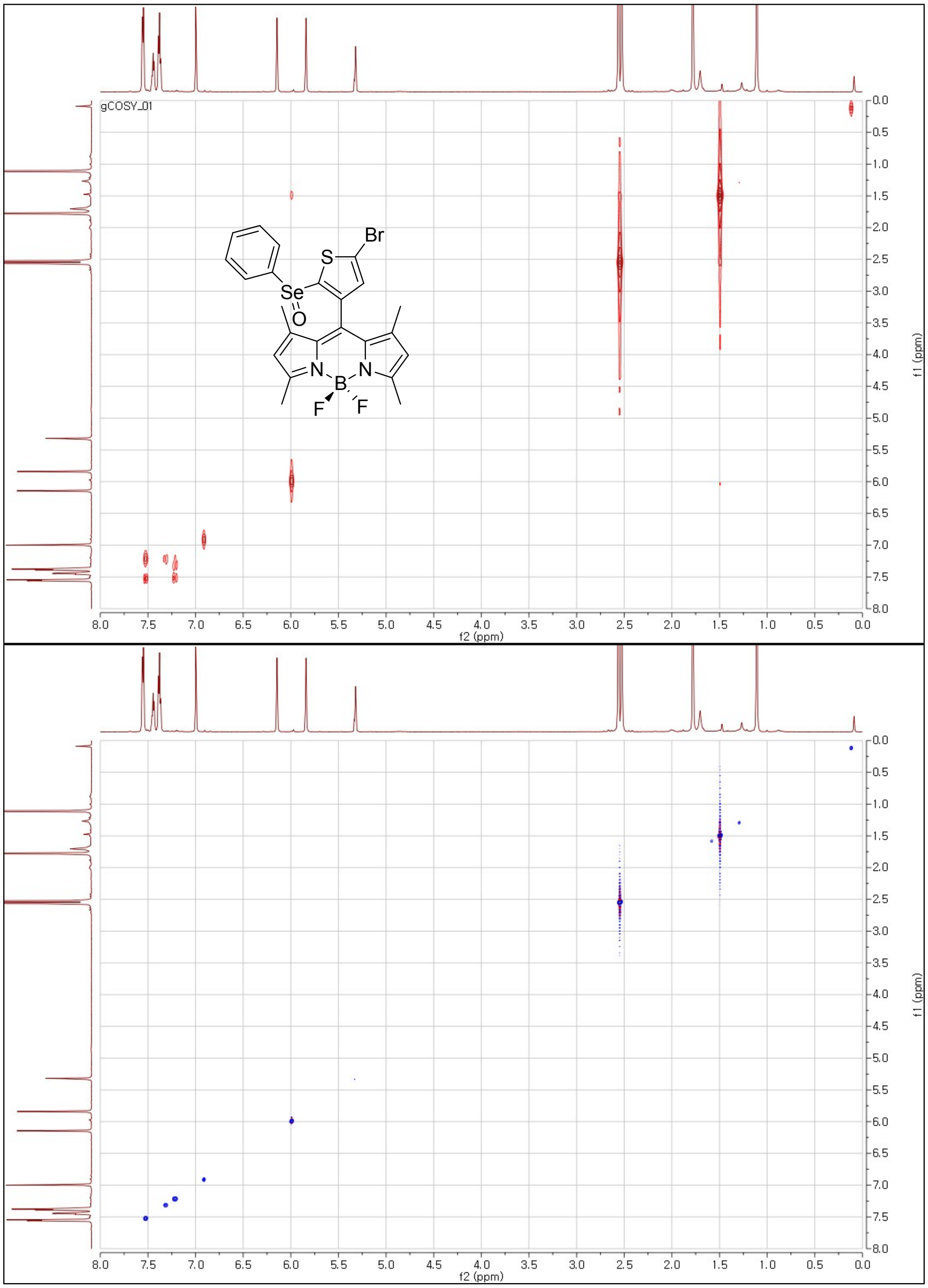

Fig. S14. (top) COSY and (bottom) NOESY spectrum of compound **4** in CD_2Cl_2.

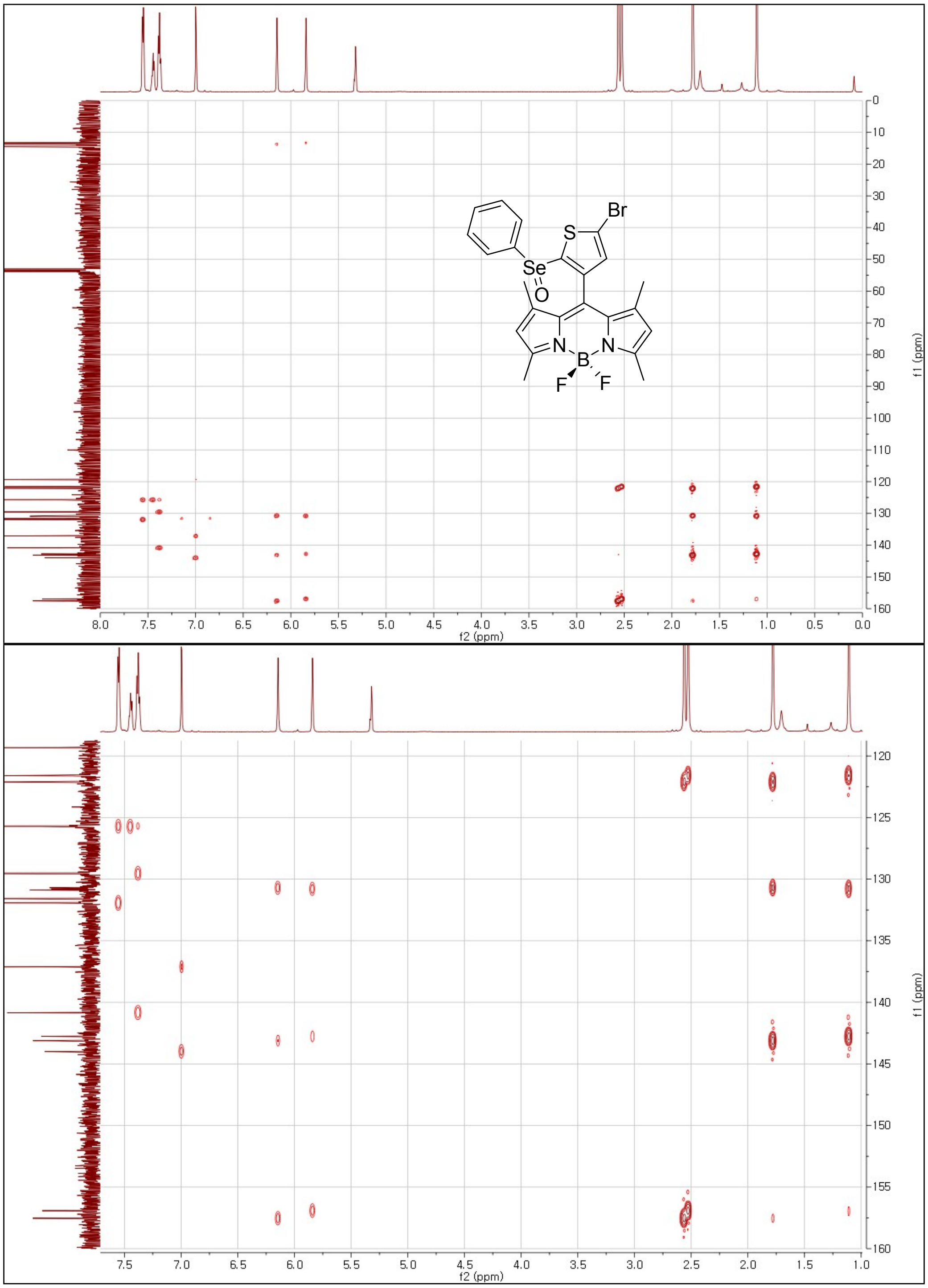

Fig. S15. (top) ^{1}H-^{13}C HMBC NMR spectrum of compound **4**, and (bottom) expanded aromatic region in CD_2Cl_2.

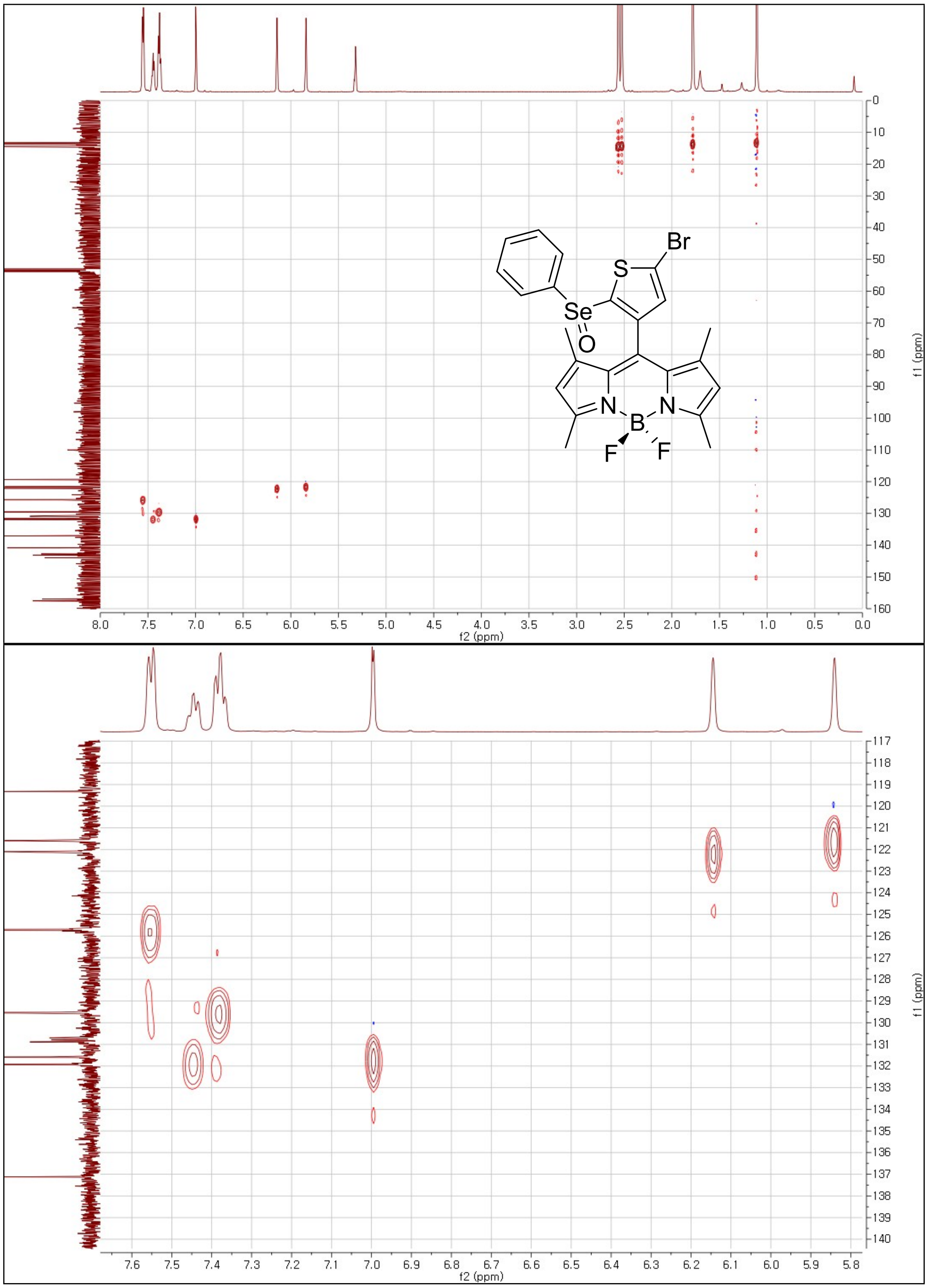

Fig. S16. (top) ^{1}H-^{13}C HSQC NMR spectrum of compound **4**, and (bottom) expanded aromatic region in CD_2Cl_2.

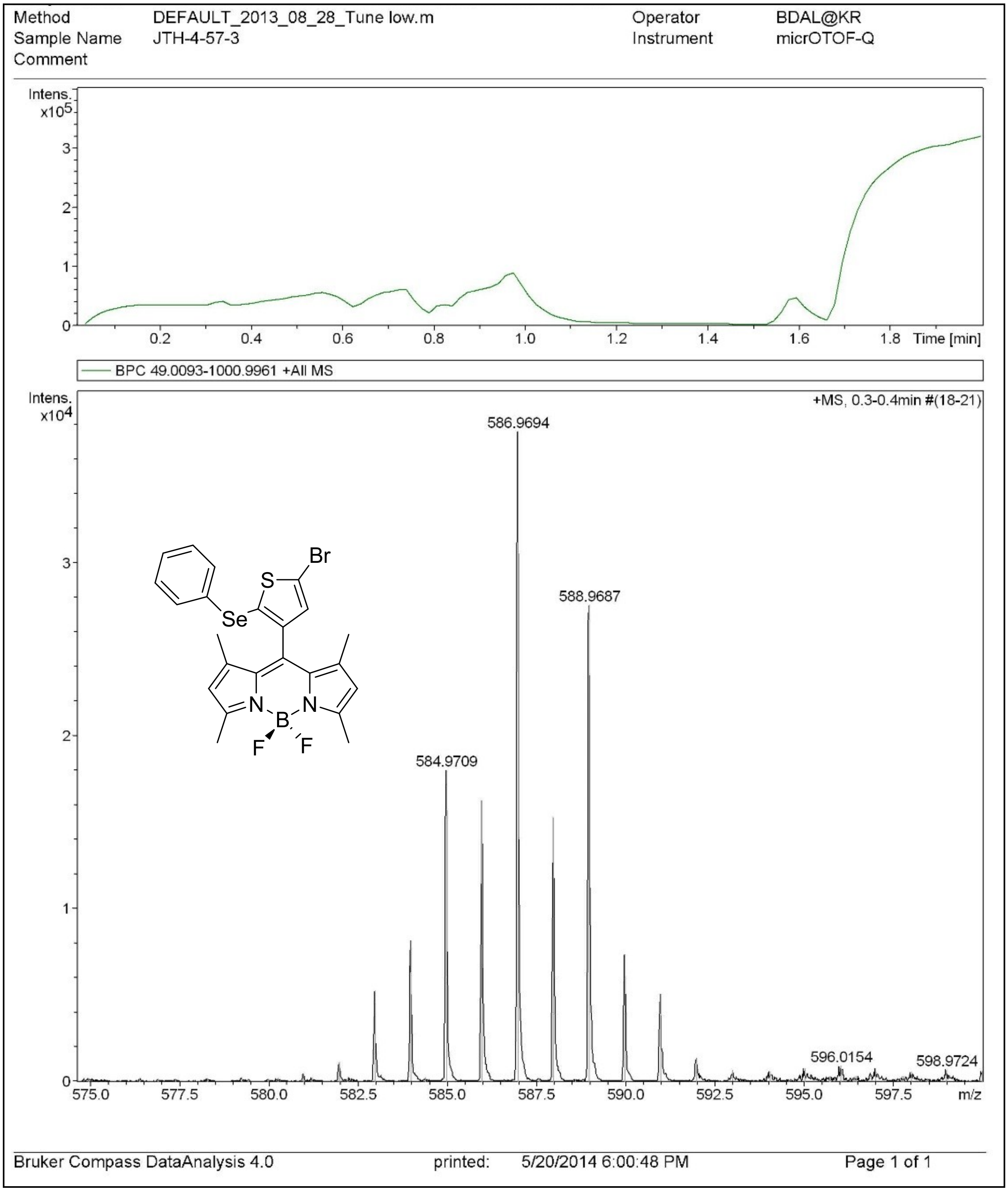

Method DEFAULT_2013_08_28_Tune low.m

Sample Name JTH-4-57-3

Comment

Operator BDAL@KR

Instrument micrOTOF-Q

Bruker Compass DataAnalysis 4.0 printed: 5/20/2014 6:00:48 PM Page 1 of 1

Fig. S17. HR-MS spectrum (ESI) of compound **3**.

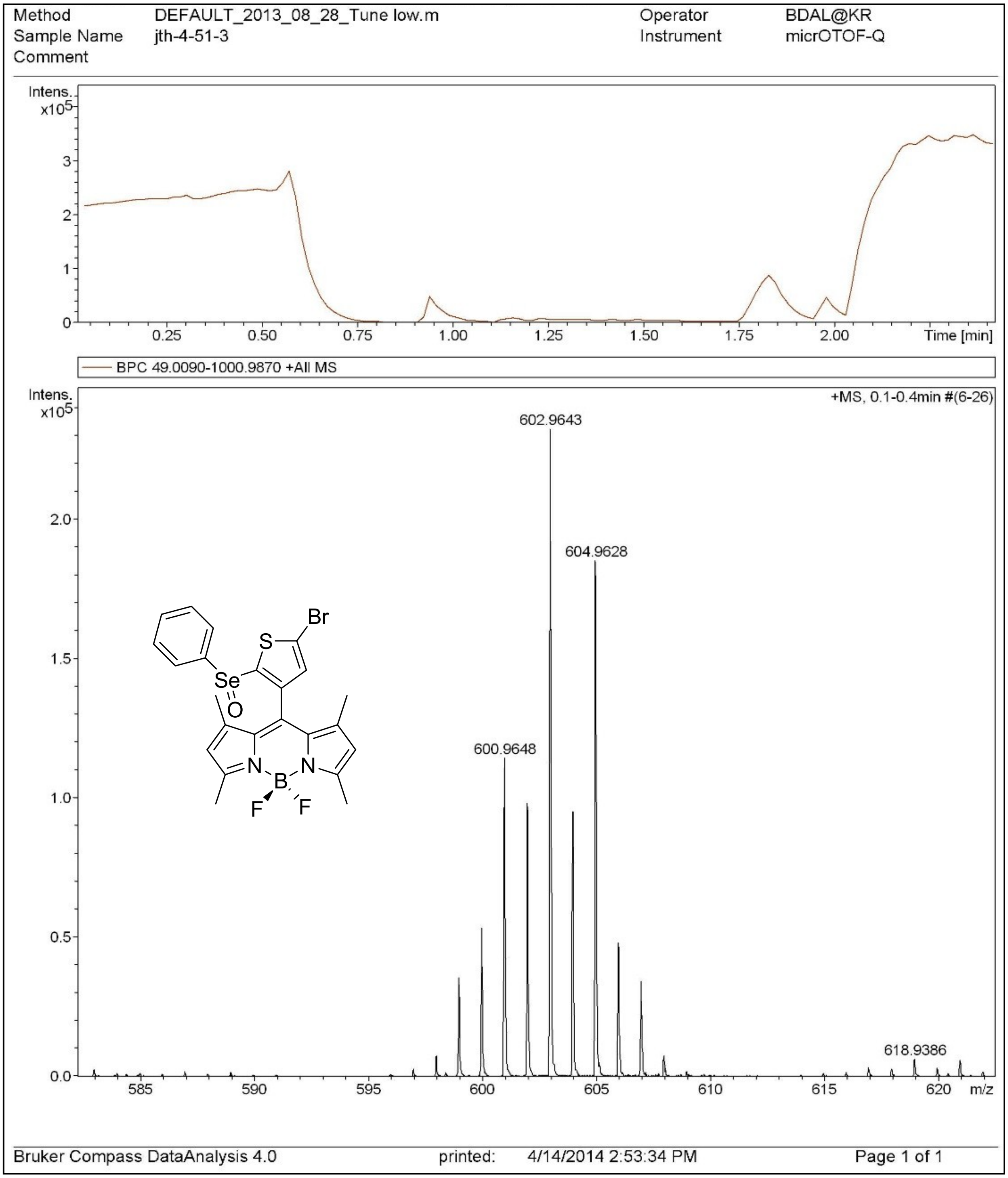

Method DEFAULT_2013_08_28_Tune low.m
Sample Name jth-4-51-3
Comment
Operator BDAL@KR
Instrument micrOTOF-Q

Bruker Compass DataAnalysis 4.0 printed: 4/14/2014 2:53:34 PM Page 1 of 1

Fig. S18. HR-MS spectrum (ESI) of compound **4**.

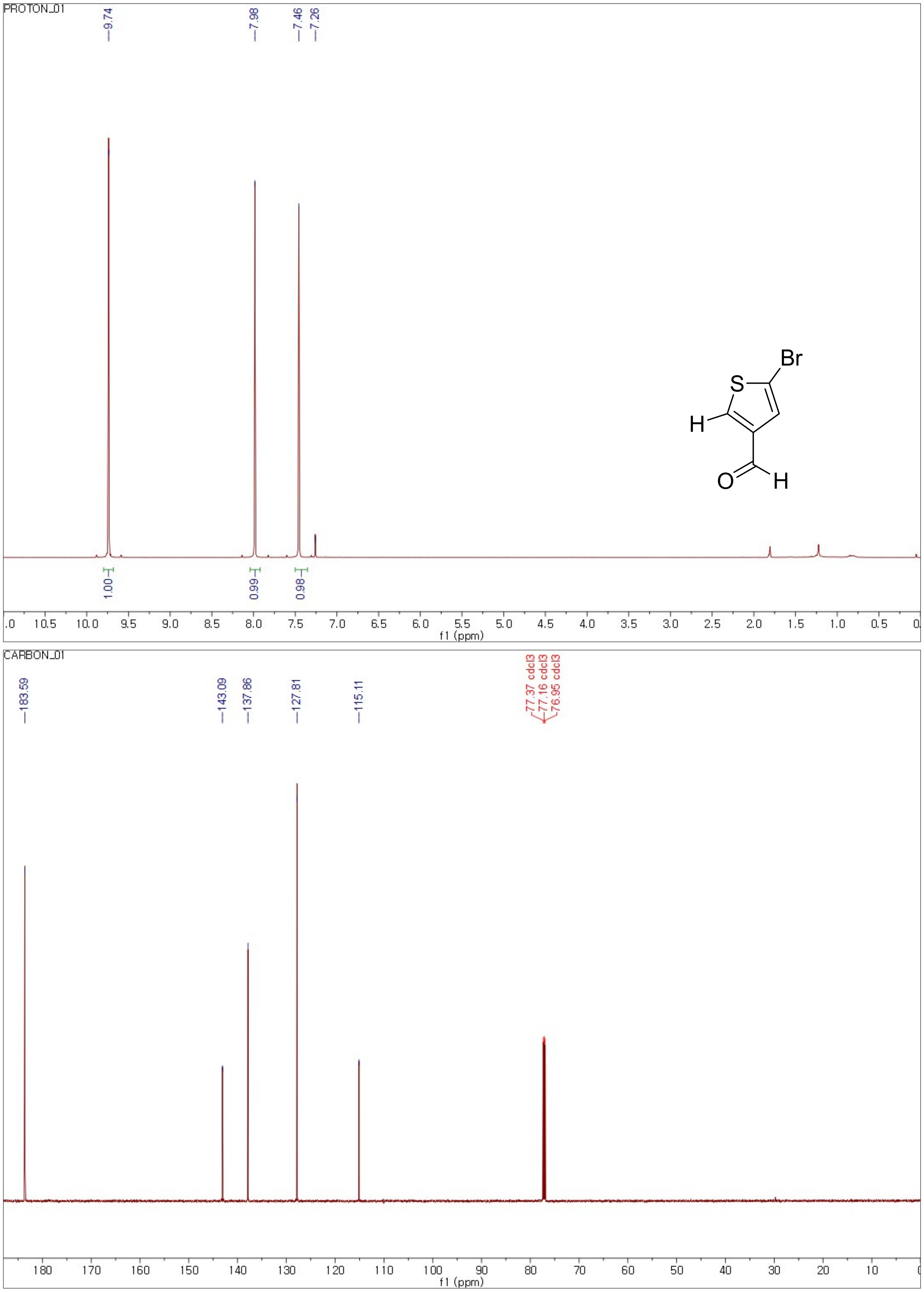

Fig. S19. (top) ^{1}H and (bottom) ^{13}C NMR spectrum of compound **5** in $CDCl_3$.

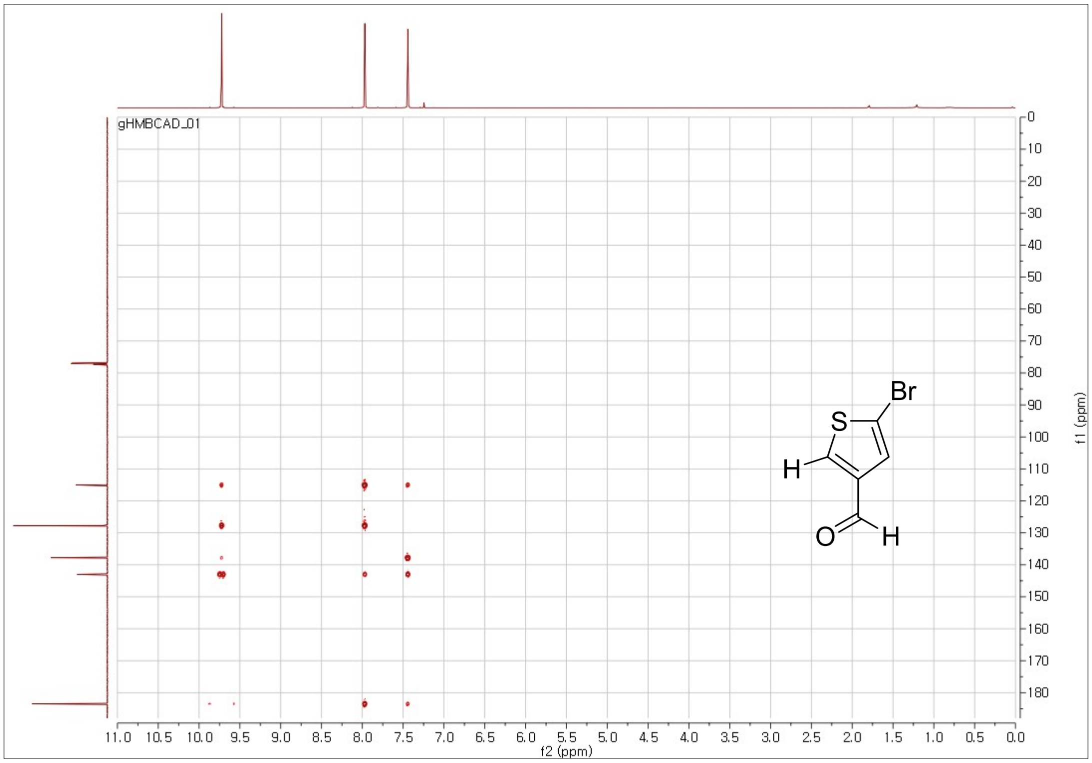

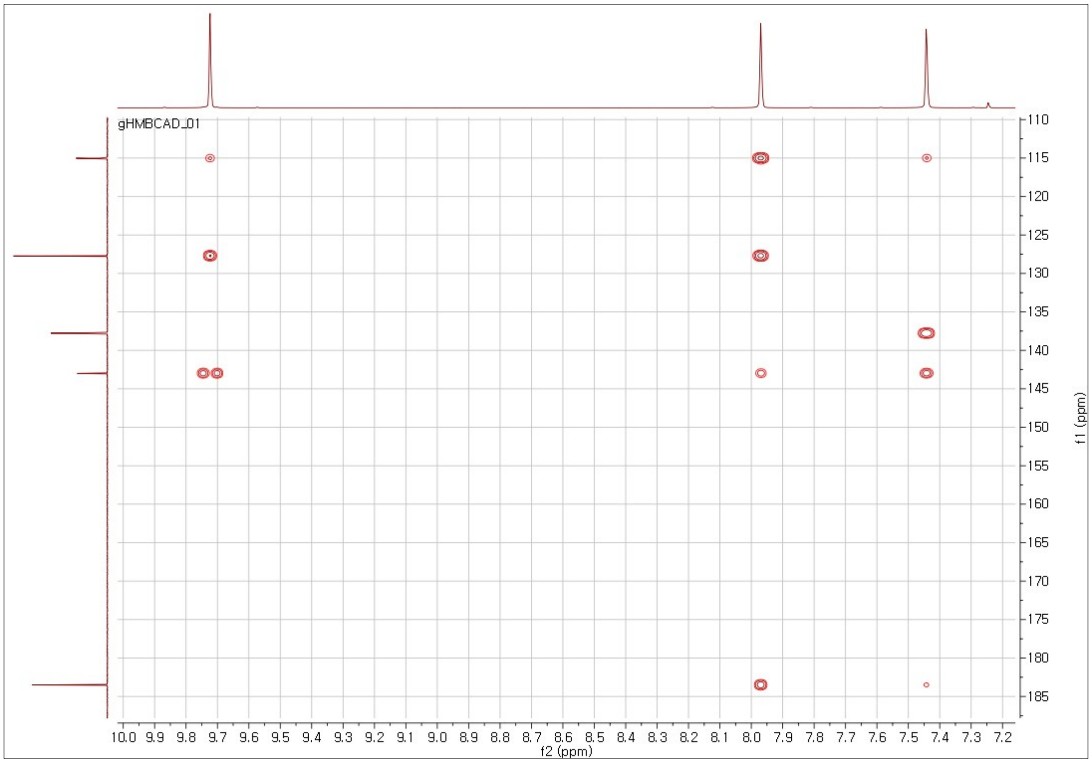

Fig. S20. (top) ^{1}H-^{13}C HMBC NMR spectrum of compound **5**, and (bottom) expanded aromatic region in $CDCl_3$.

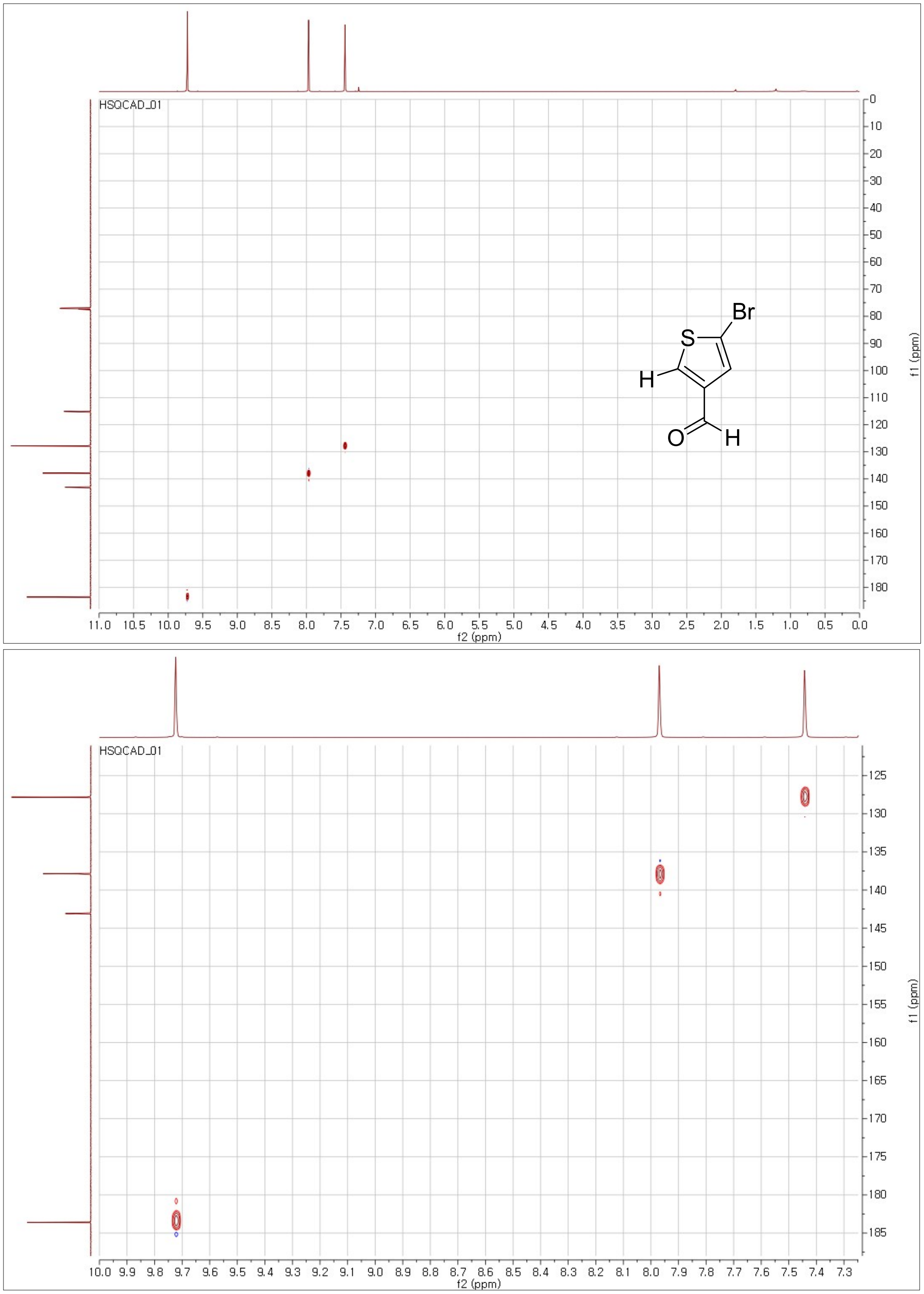

Fig. S21. (top) ^{1}H-^{13}C HSQC NMR spectrum of compound **5**, and (bottom) expanded aromatic region in $CDCl_3$.

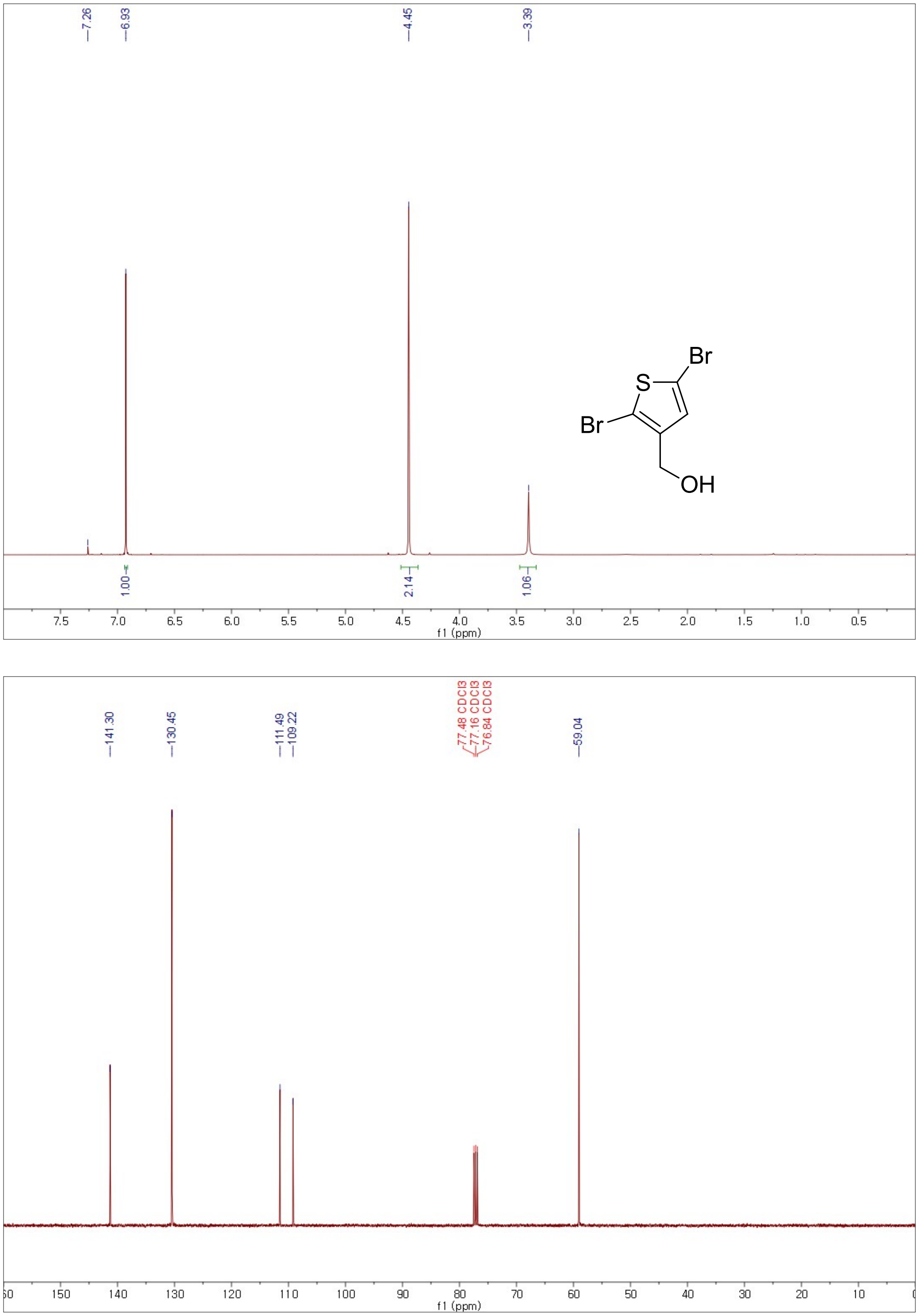

Fig. S22. (top) ^{1}H and (bottom) ^{13}C NMR spectrum of compound **7** in $CDCl_3$.

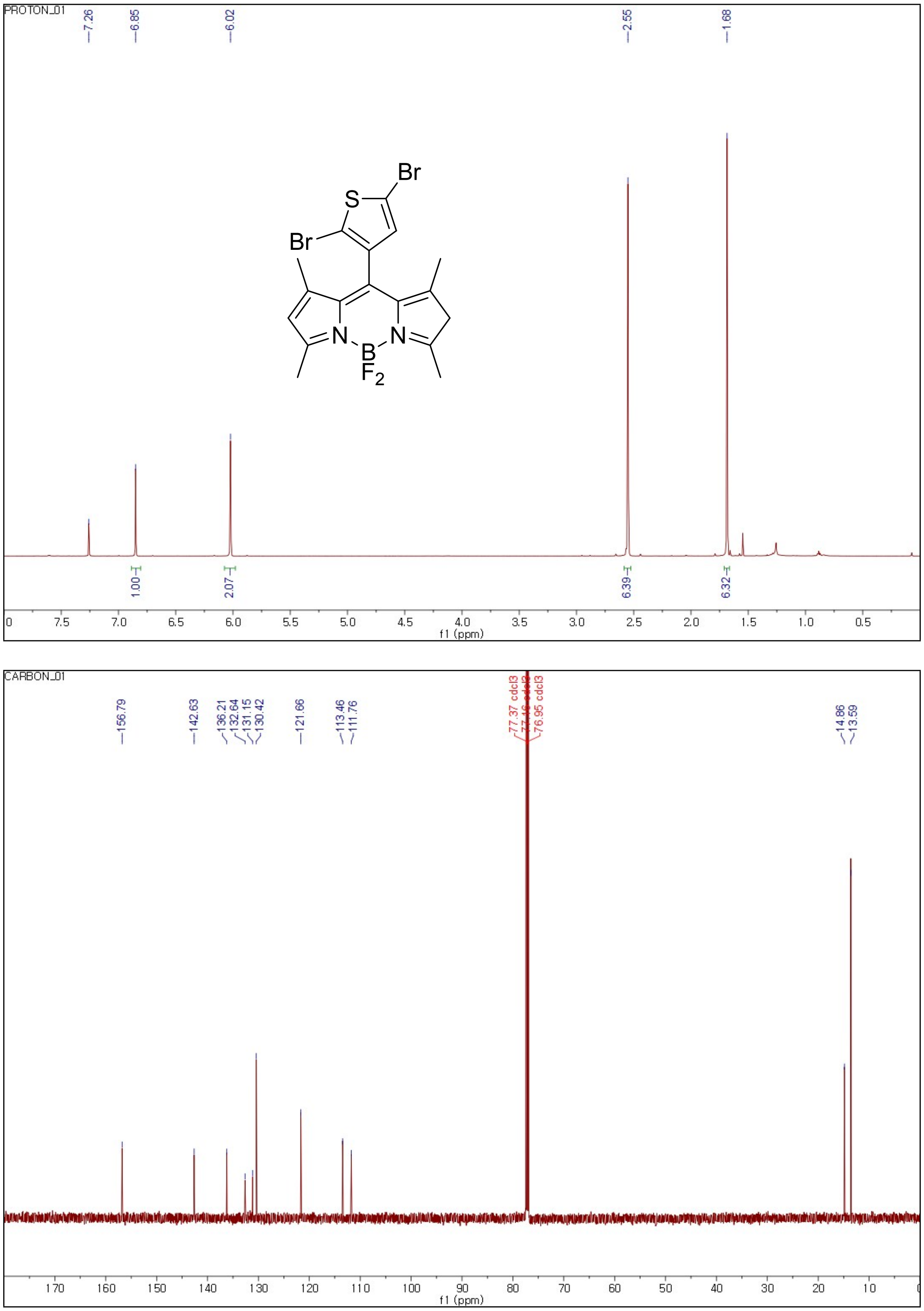

Fig. S23. (top) ^{1}H and (bottom) ^{13}C NMR spectrum of compound **8** in $CDCl_3$.

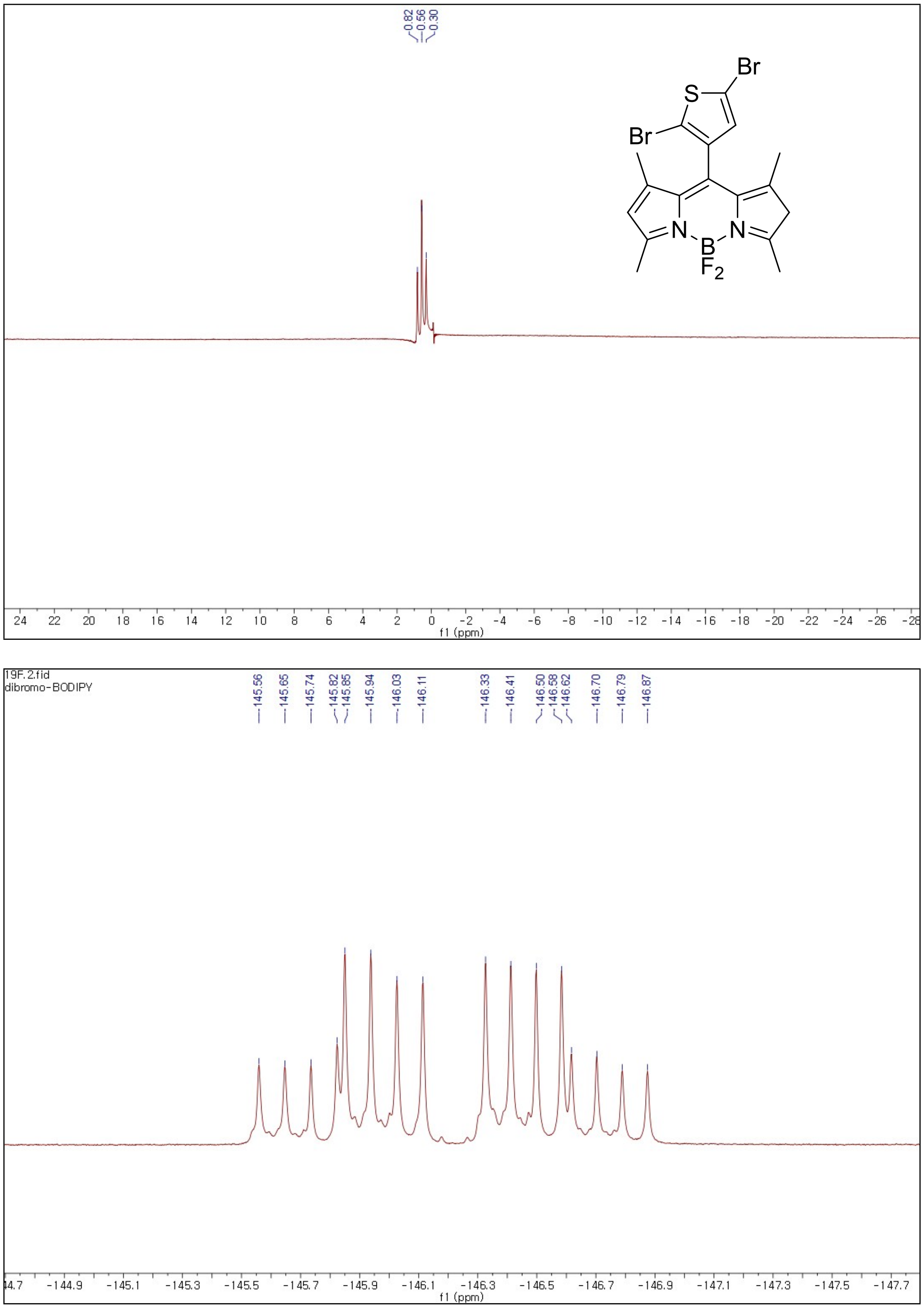

Fig. S24. (top) ^{11}B and (bottom) ^{19}F NMR spectrum of compound **8** in CDCl$_3$.

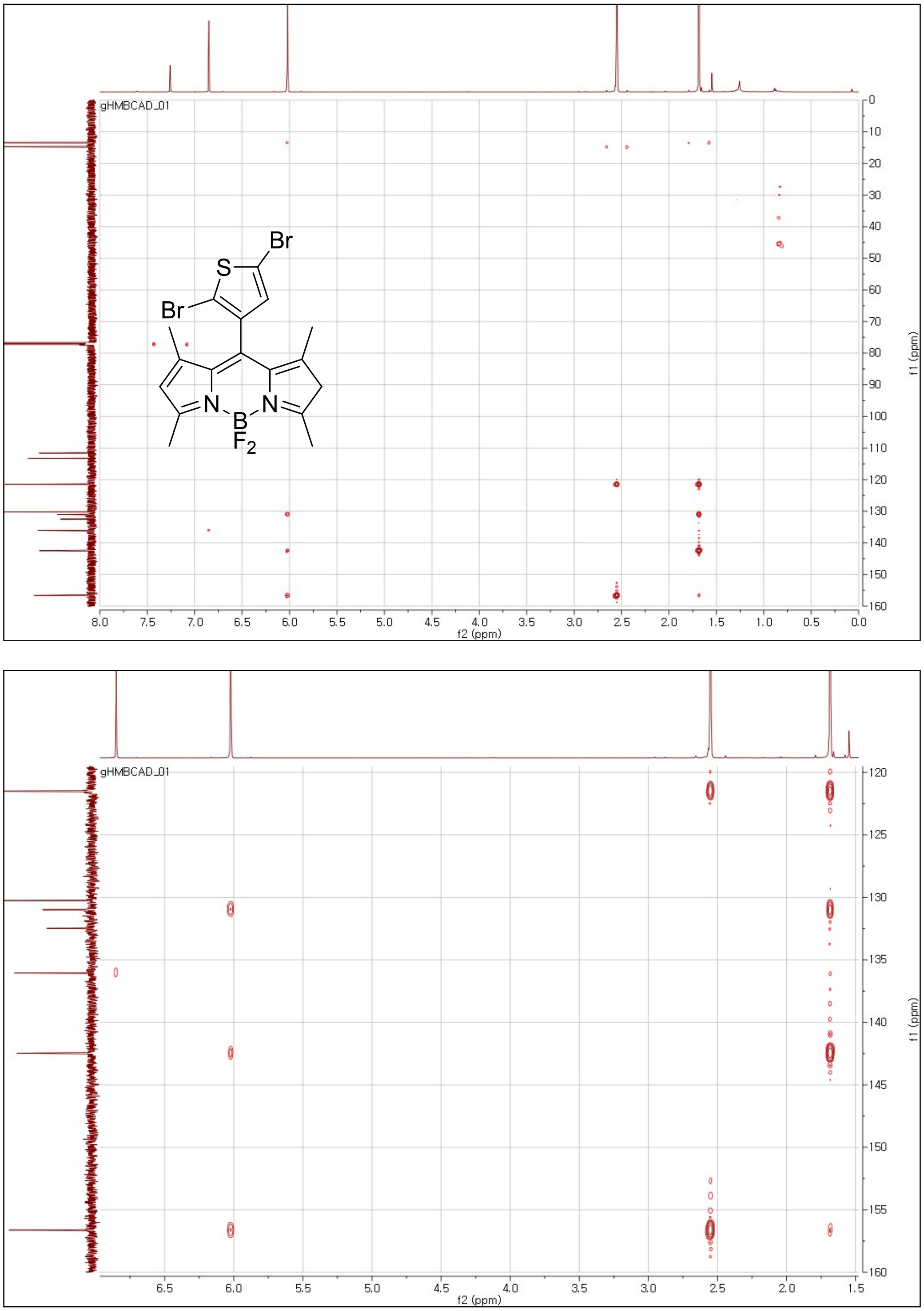

Fig. S25. (top) ^{1}H-^{13}C HMBC NMR spectrum of compound **8**, and (bottom) expanded aromatic region in $CDCl_3$.

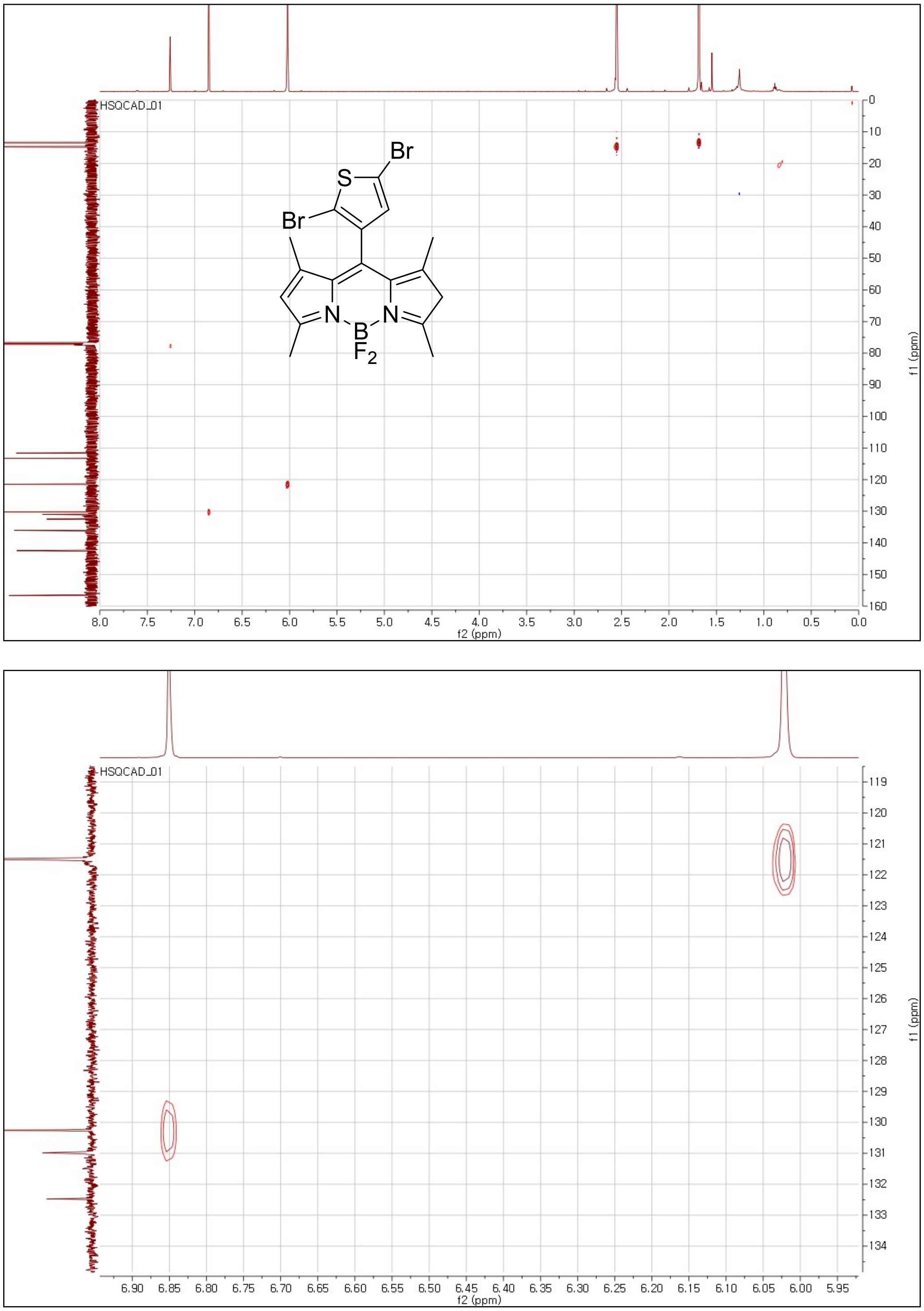

Fig. S26. (top) ^{1}H-^{13}C HSQC NMR spectrum of compound **8**, and (bottom) expanded aromatic region in $CDCl_3$.

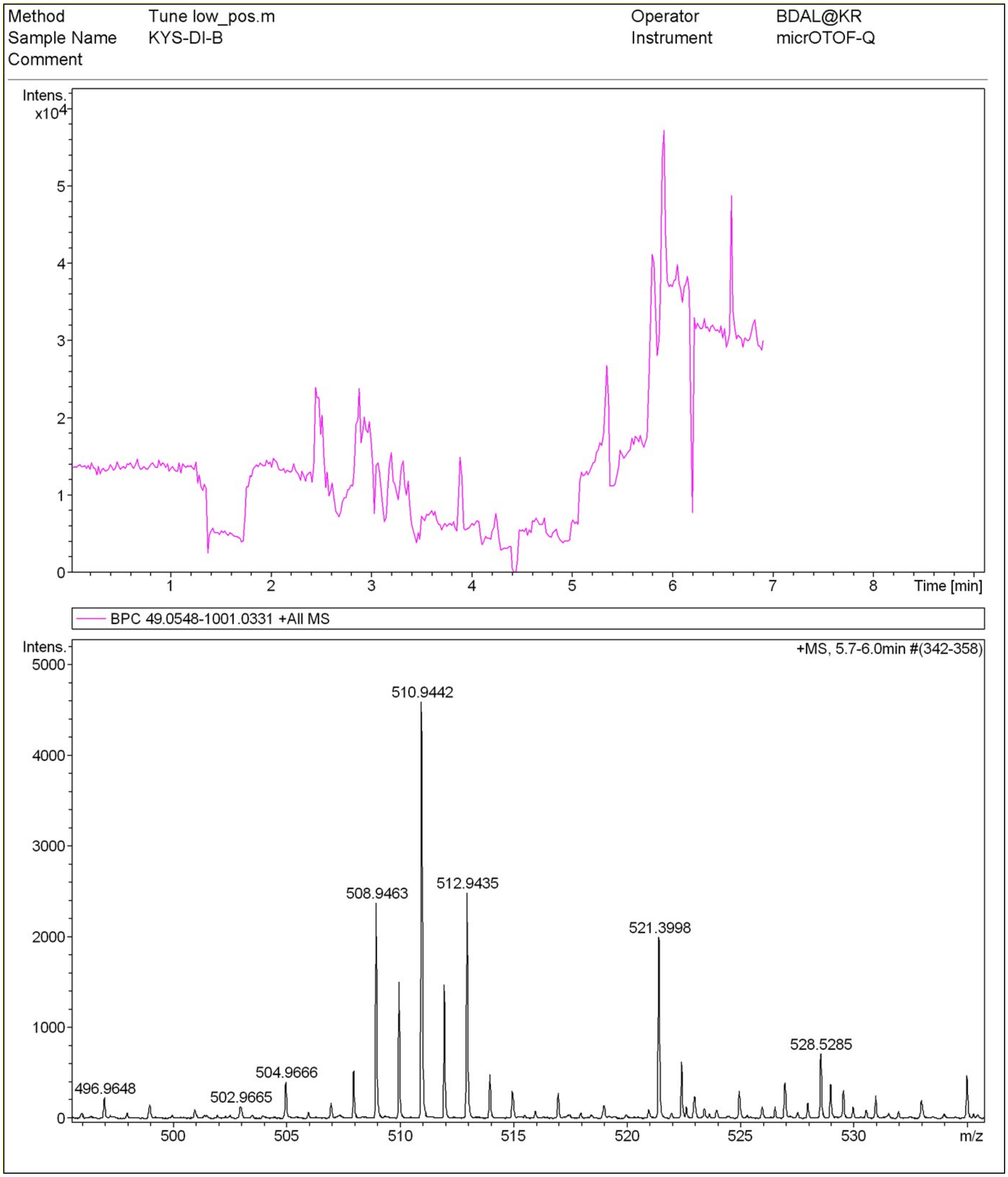

Method	Tune low_pos.m	Operator	BDAL@KR
Sample Name	KYS-DI-B	Instrument	micrOTOF-Q
Comment			

Fig. S27. HR-MS spectrum (ESI) of compound **8**.

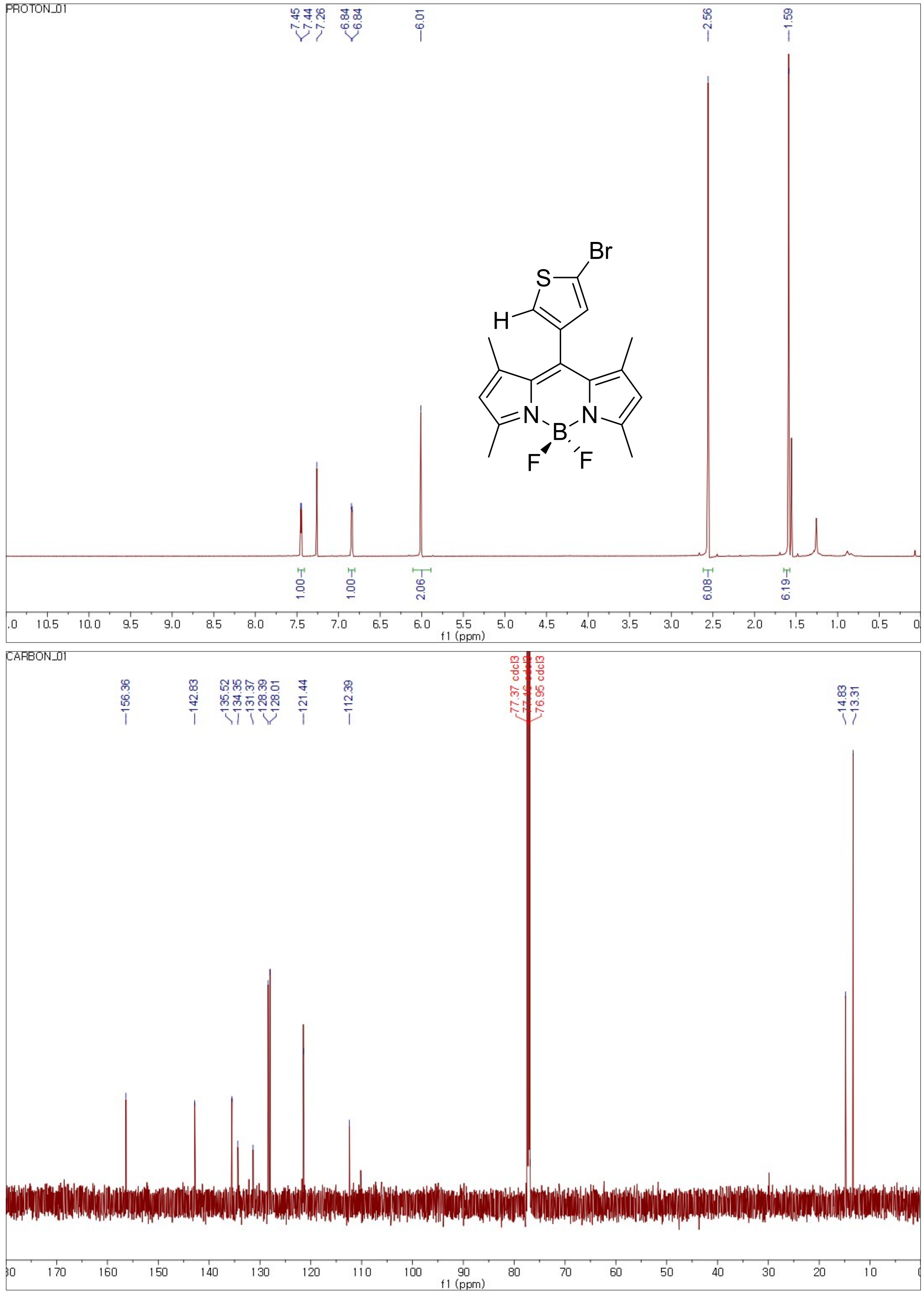

Fig. S28. (top) ^{1}H and (bottom) ^{13}C NMR spectrum of compound **9** in $CDCl_3$.

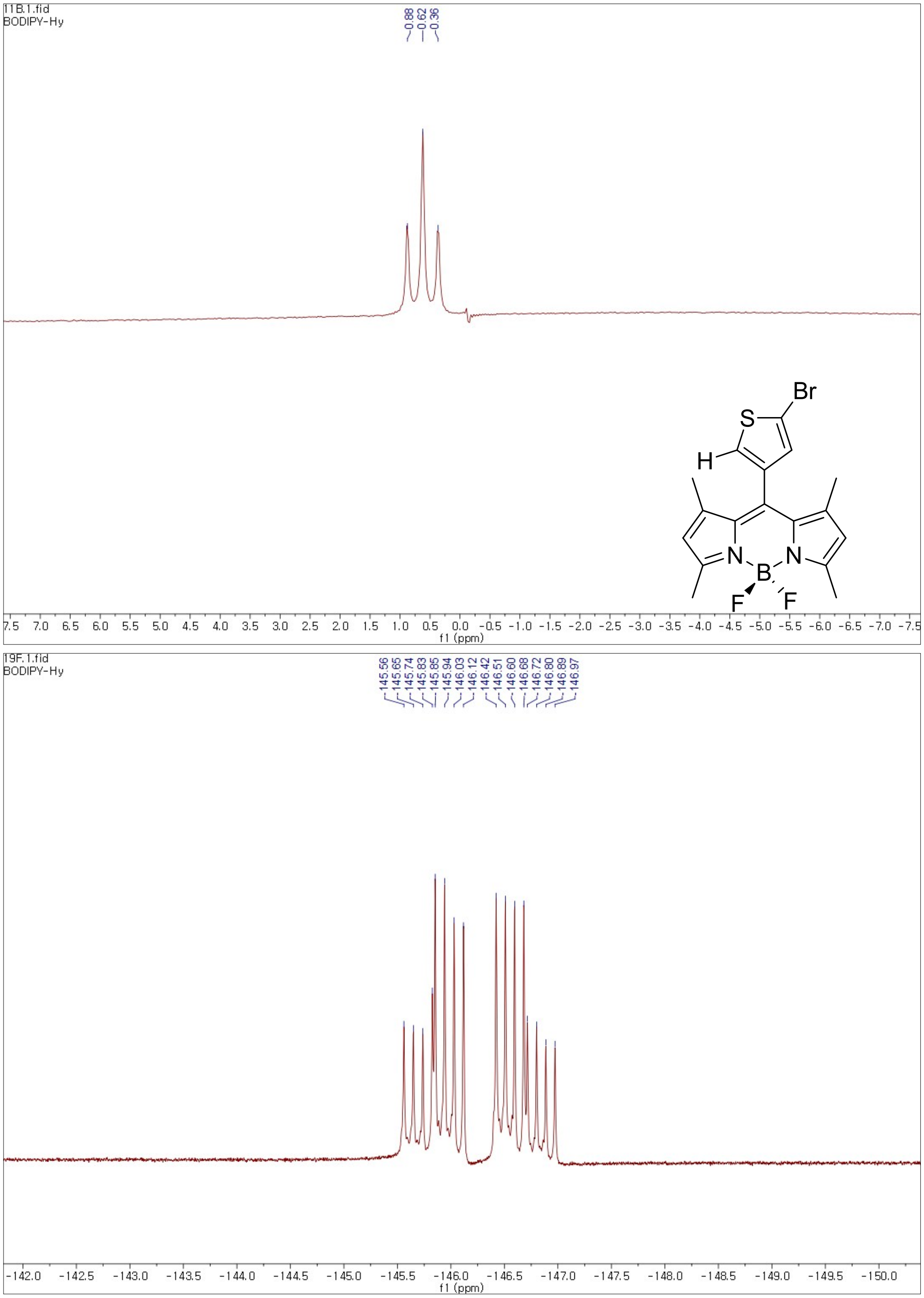

Fig. S29. (top) ^{11}B and (bottom) ^{19}F NMR spectrum of compound **9** in CDCl$_3$.

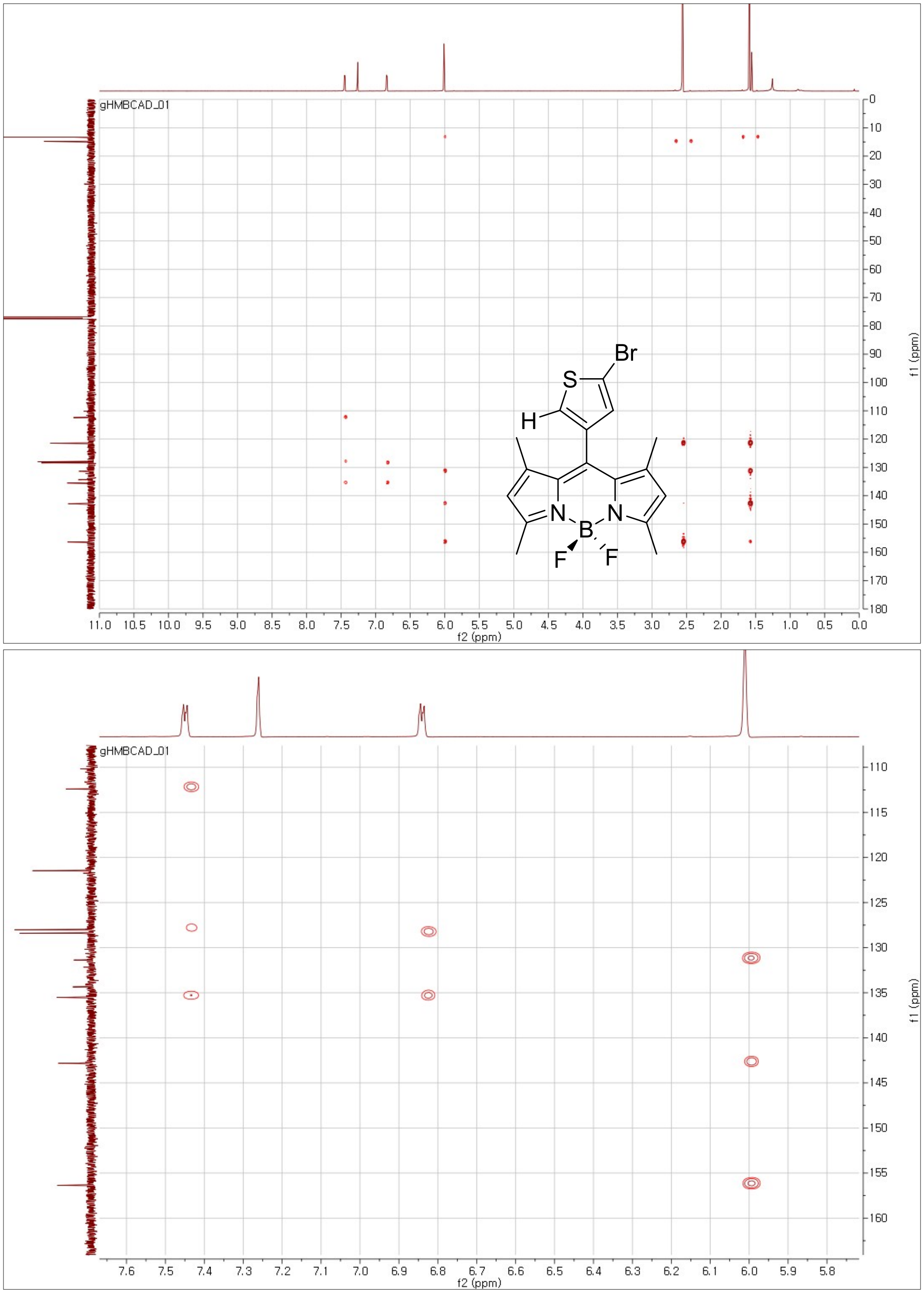

Fig. S30. (top) ^1H-^{13}C HMBC NMR spectrum of compound **9**, and (bottom) expanded aromatic region in $CDCl_3$.

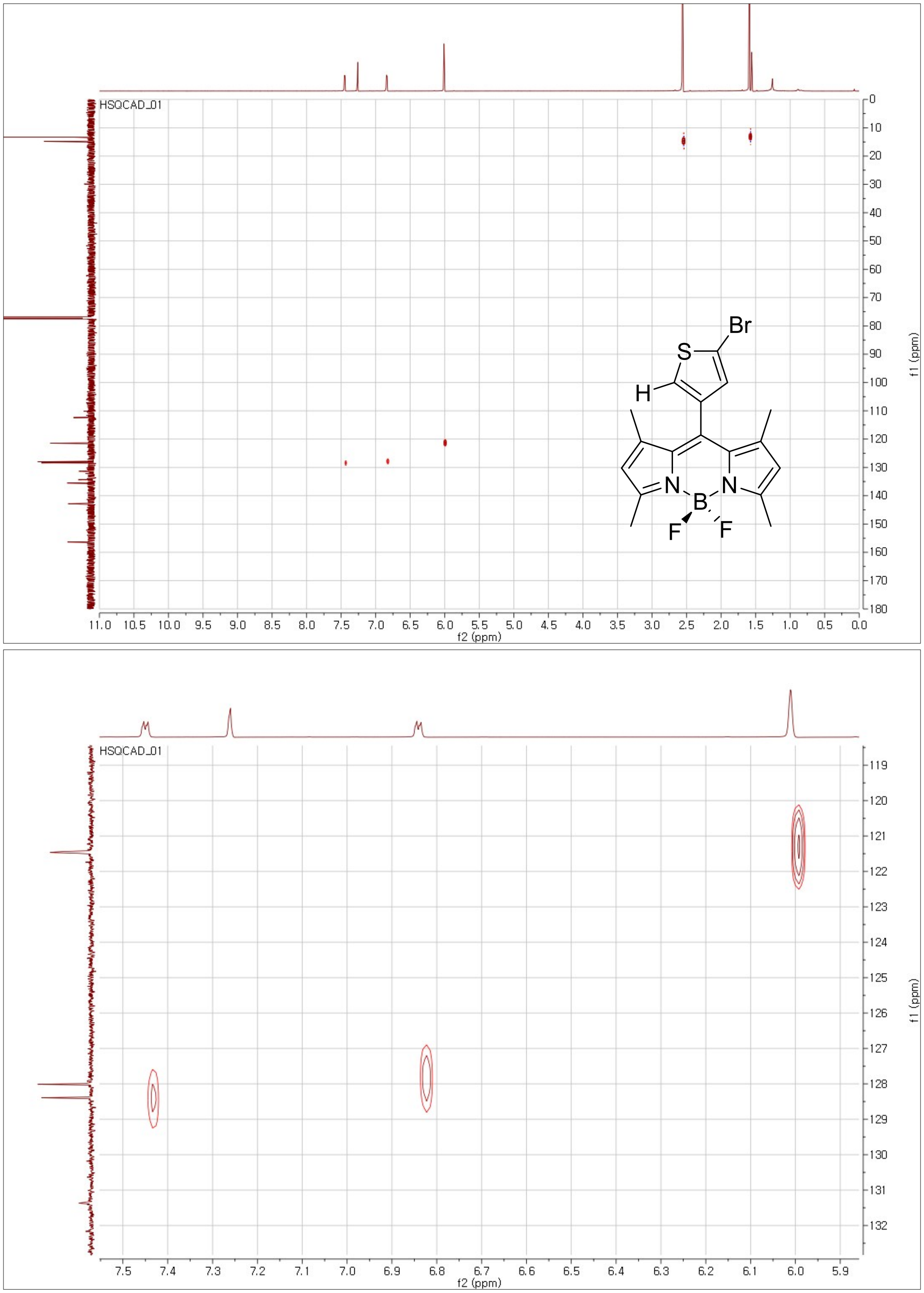

Fig. S31. (top) ^{1}H-^{13}C HSQC NMR spectrum of compound **9**, and (bottom) expanded aromatic region in $CDCl_3$.

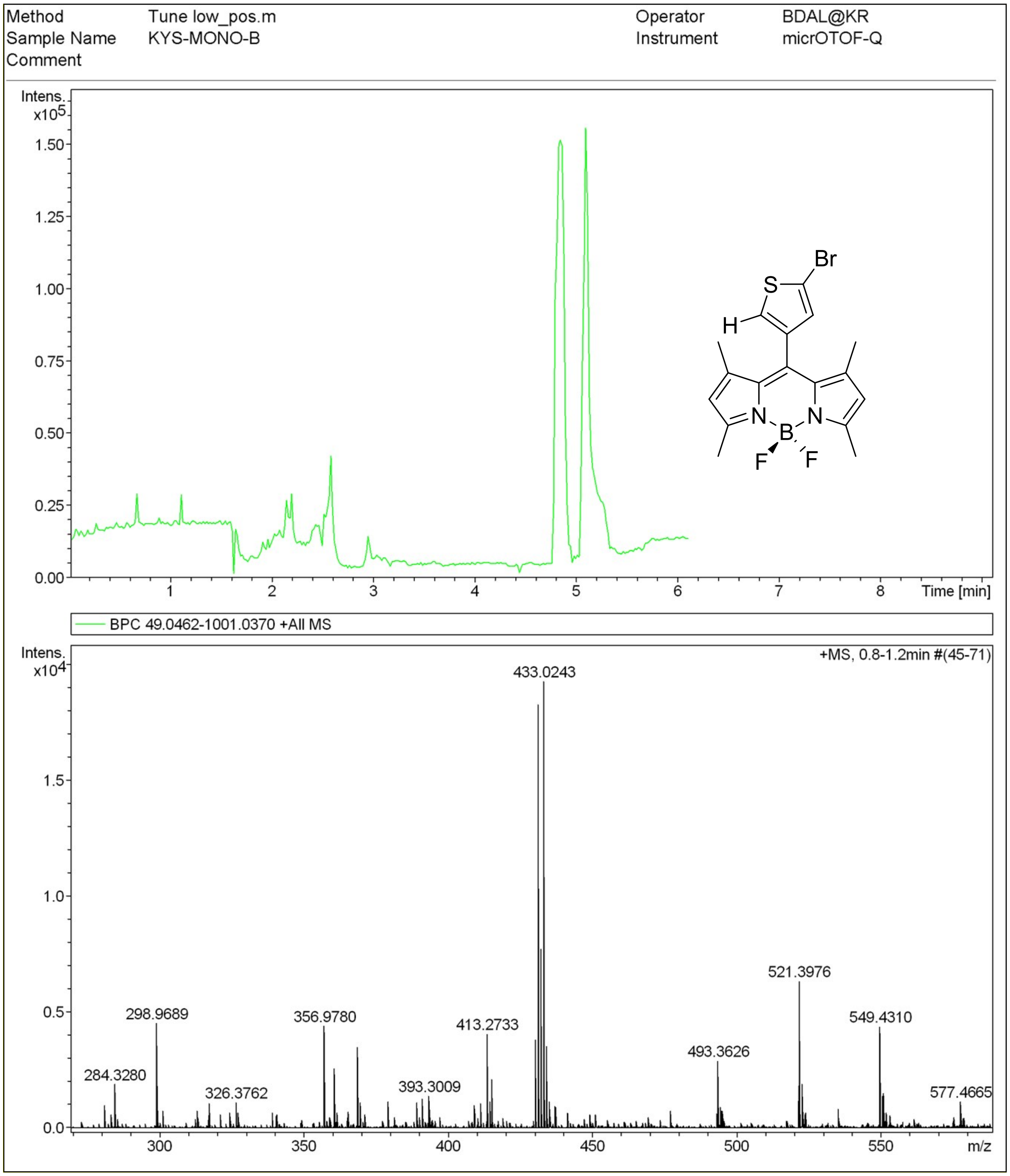

Method	Tune low_pos.m	Operator	BDAL@KR
Sample Name	KYS-MONO-B	Instrument	micrOTOF-Q
Comment			

Fig. S32. HR-MS spectrum (ESI) of compound **9**.

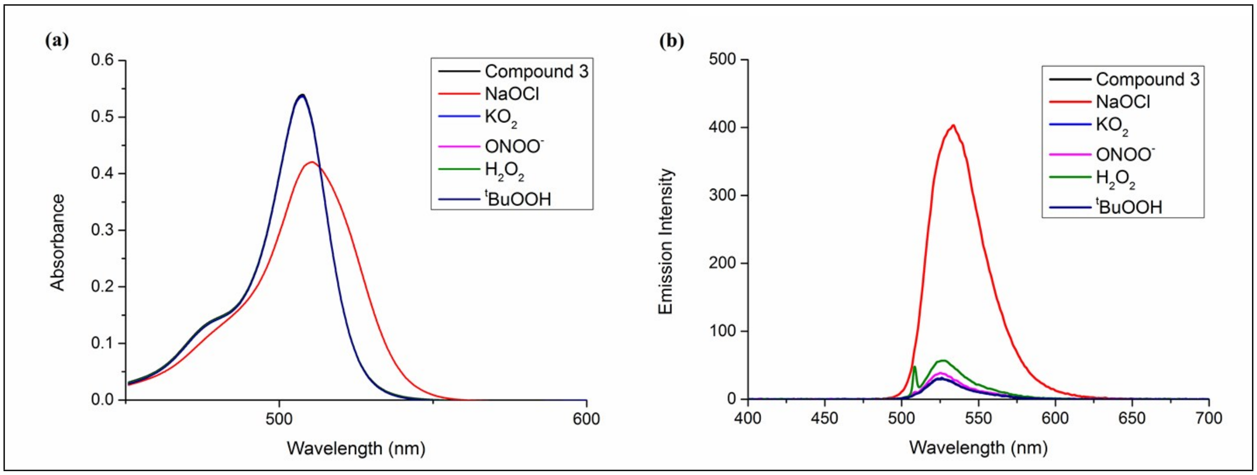

Fig. S33. (a) UV–absorption spectra of compound **3** (10.0 µM) with 5.0 equiv ROS (KO_2, H_2O_2, ^{t}BuOOH, NaOCl, $ONOO^-$) in the solution (CH_3CN:H_2O, 1:1 v/v); (b) Fluorescence spectra of compound **3** (10.0 µM) with 5.0 equiv ROS (KO_2, H_2O_2, ^{t}BuOOH, NaOCl, $ONOO^-$) in the solution (CH_3CN:H_2O, 1:1 v/v), Slit width for Ex. and Em. = 1.5 nm

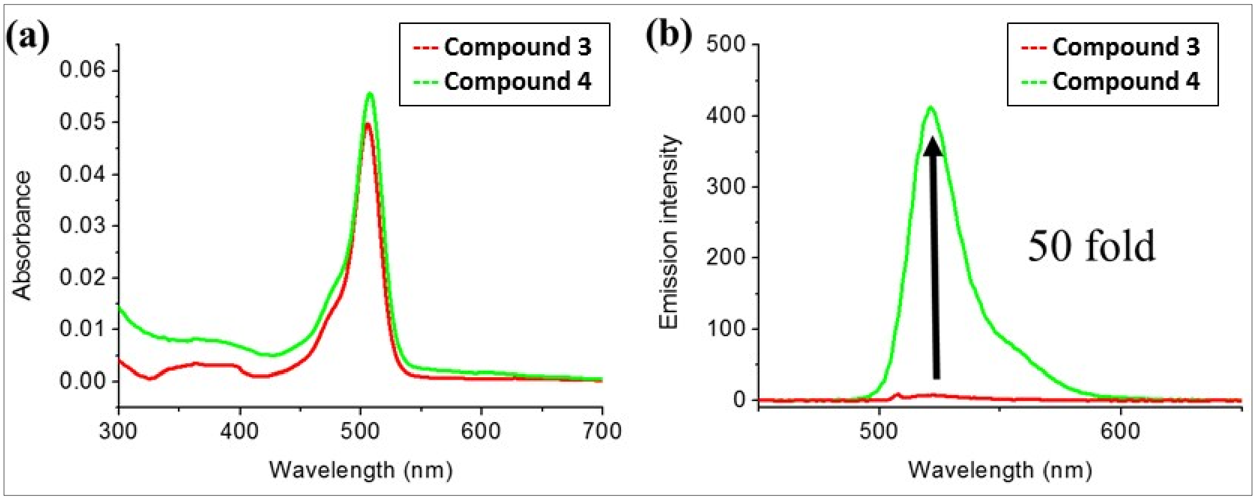

Fig. S34. (a) UV–absorption spectra of compound **3** (10.0 µM) and **4** (1.0 µM) in CH_3CN; (b) Fluorescence spectra of compound **3** (1.0 µM) and **4** (10.0 µM) in CH_3CN; Slit width for Ex. and Em. = 1.5 nm.

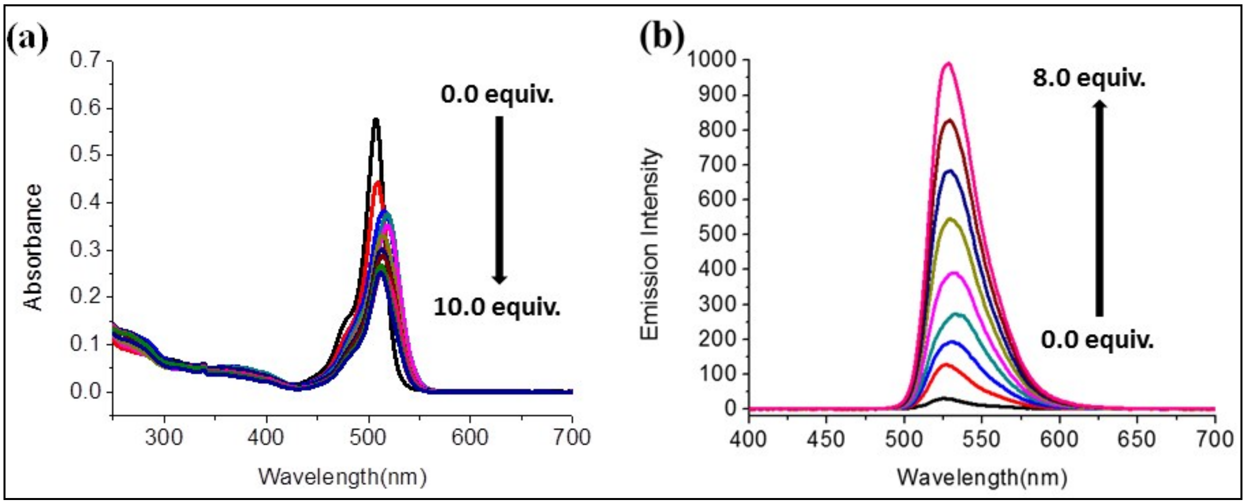

Fig. S35. (a) UV–absorption spectra of compound **3** (10.0 μM) with 0 to 10.0 equiv of NaOCl in the solution ($CH_3CN:H_2O$, 1:1 v/v); (b) Fluorescence spectra of compound **3** (10.0 μM) with 0.0 to 8.0 equiv of NaOCl in the solution ($CH_3CN:H_2O$, 1:1 v/v). Slit width for Ex. and Em. = 1.5 nm.

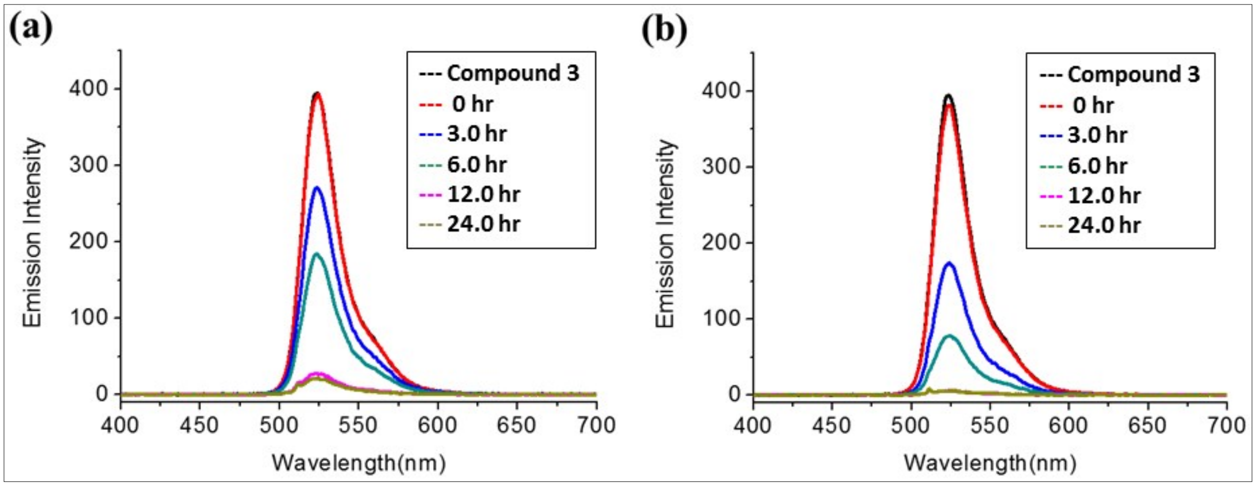

Fig. S36. (a) Fluorescence spectra of compound **4** (1 μM) with GSH (500 equiv, 0-24 hr) in the solution ($CH_3CN:H_2O$, 1:1 v/v), Slit width for Ex. and Em. = 1.5 nm; (b) Fluorescence spectra of compound **4** (1.0 μM) with GSH (1000 equiv, 0-24 hr) in the solution ($CH_3CN:H_2O$, 1:1 v/v), Slit width for Ex. and Em. = 1.5 nm.

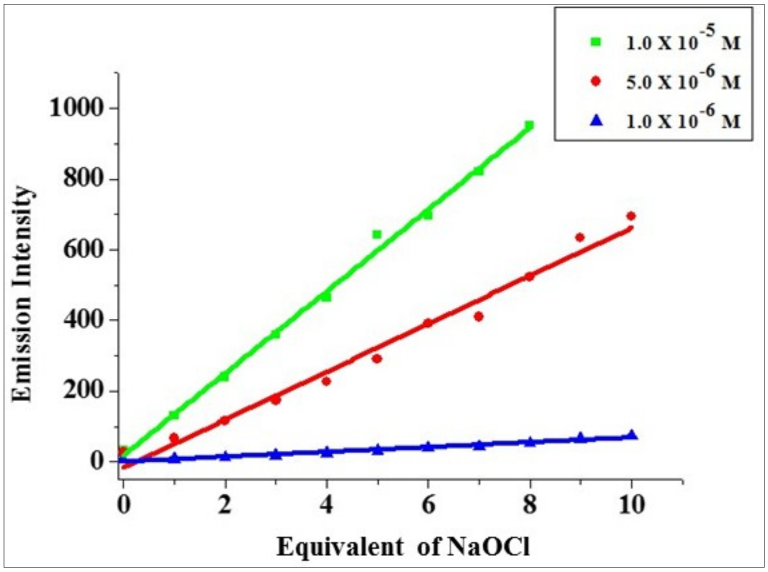

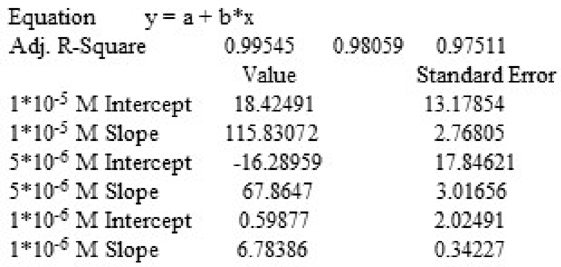

Equation	y = a + b*x		
Adj. R-Square	0.99545	0.98059	0.97511
	Value		Standard Error
$1*10^{-5}$ M Intercept	18.42491		13.17854
$1*10^{-5}$ M Slope	115.83072		2.76805
$5*10^{-6}$ M Intercept	-16.28959		17.84621
$5*10^{-6}$ M Slope	67.8647		3.01656
$1*10^{-6}$ M Intercept	0.59877		2.02491
$1*10^{-6}$ M Slope	6.78386		0.34227

Fig. S37. Titration curves of compound **3** (1.0 µM, 5.0 µM, 10.0 µM) with increasing equivalents of NaOCl added to the solution ($CH_3CN:H_2O$, 1:1 v/v), Slit width for Ex. and Em. = 1.5 nm.

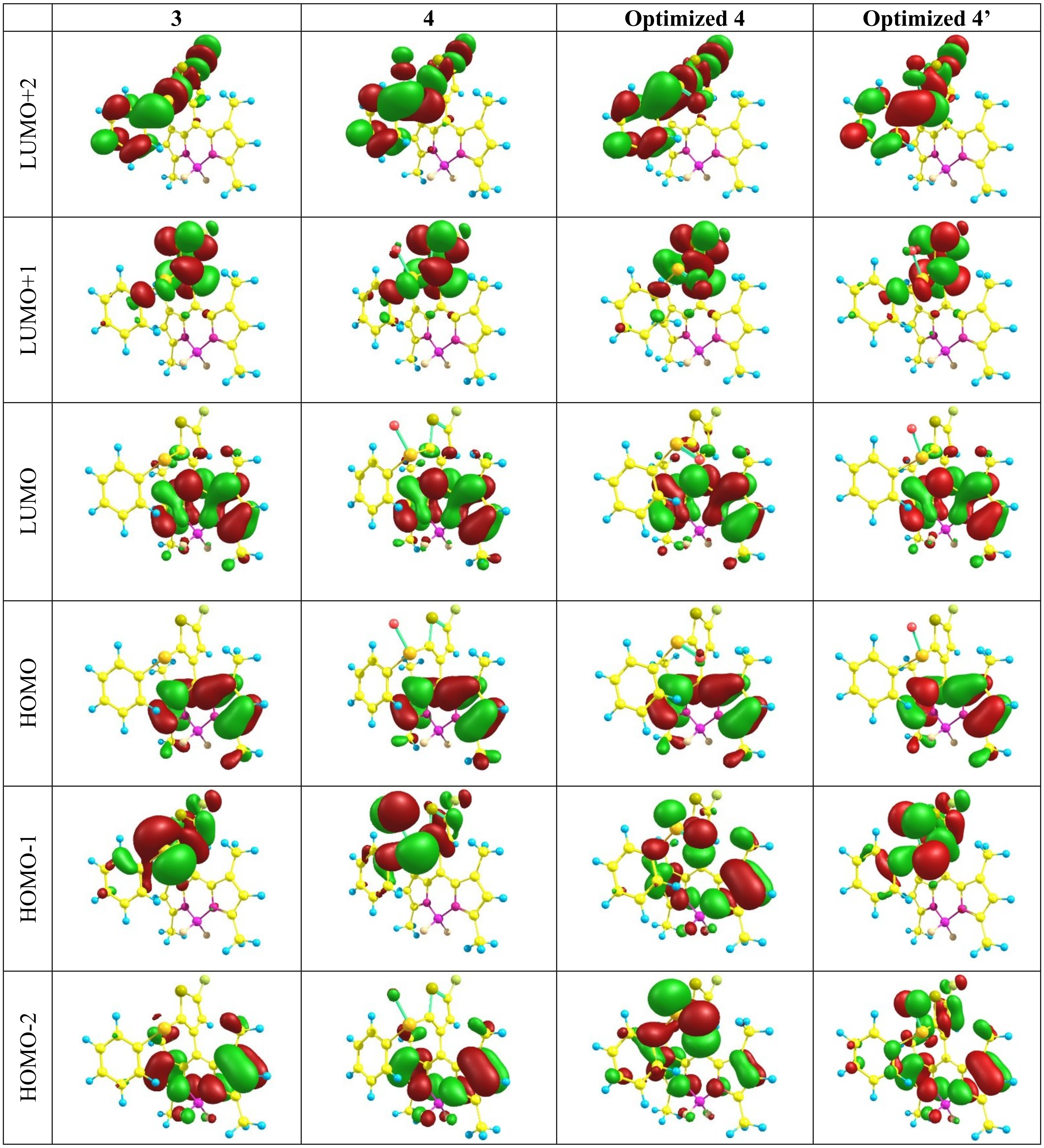

Fig. S38. From LUMO + 2 to HOMO −2 (from top to bottom) of geometry–optimized compound **3**, compound **4** and **optimized 4/4’**(left to right) based on gas phase calculations.

Table S1. Crystal data and structure refinement for compound **4**.

CCDC No.	1000278	
Empirical formula	C23 H20 B Br F2 N2 O S Se	
Formula weight	580.15	
Temperature	293(2) K	
Wavelength	0.71073 Å	
Crystal system	Triclinic	
Space group	P-1	
Unit cell dimensions	*a* = 8.9526(2) Å	α = 94.4778(14)°.
	b = 10.2532(3) Å	β = 106.8774(12)°.
	c = 14.7976(4) Å	γ = 114.9387(12)°.
Volume	1146.72(5) Å^3	
Z	2	
Density (calculated)	1.680 Mg/m^3	
Absorption coefficient	3.506 mm^{-1}	
F(000)	576	
Crystal size	0.30 × 0.18 × 0.03 mm^3	
Theta range for data collection	2.75 to 28.06°.	
Index ranges	$-11 \leq h \leq 11$, $-13 \leq k \leq 13$, $-19 \leq l \leq 19$	
Reflections collected	63841	
Independent reflections	5542 [R(int) = 0.0414]	
Completeness to theta = 28.06°	99.4 %	
Absorption correction	Semi-empirical from equivalents	
Max. and min. transmission	0.9021 and 0.4194	
Refinement method	Full-matrix least-squares on F^2	
Data / restraints / parameters	5542 / 0 / 289	
Goodness-of-fit on F^2	1.075	
Final R indices [I>2sigma(I)]	R1 = 0.0363, wR2 = 0.0935	
R indices (all data)	R1 = 0.0466, wR2 = 0.0989	
Largest diff. peak and hole	0.852 and -0.388 e.Å^{-3}	

Table S2. Bond lengths [Å] and angles [°] for compound **4**.

Se(1)-O(1)	1.6602(19)
Se(1)-C(17)	1.928(2)
Se(1)-C(18)	1.932(3)
Br(1)-C(16)	1.871(3)
S(1)-C(16)	1.712(3)
S(1)-C(17)	1.719(2)
B(1)-F(2)	1.385(3)
B(1)-F(1)	1.391(4)
B(1)-N(1)	1.540(5)
B(1)-N(2)	1.543(5)
N(1)-C(2)	1.348(4)
N(1)-C(6)	1.402(3)
N(2)-C(8)	1.342(4)
N(2)-C(12)	1.404(3)
C(1)-C(2)	1.503(4)
C(2)-C(3)	1.388(5)
C(3)-C(4)	1.378(4)
C(4)-C(6)	1.422(4)
C(4)-C(5)	1.505(4)
C(6)-C(13)	1.392(4)
C(7)-C(8)	1.504(5)
C(8)-C(9)	1.385(6)
C(9)-C(10)	1.381(4)
C(10)-C(12)	1.423(4)
C(10)-C(11)	1.485(5)
C(12)-C(13)	1.389(4)
C(13)-C(14)	1.484(3)
C(14)-C(17)	1.359(3)
C(14)-C(15)	1.424(4)
C(15)-C(16)	1.352(4)
C(18)-C(23)	1.371(5)
C(18)-C(19)	1.375(4)
C(19)-C(20)	1.382(5)
C(20)-C(21)	1.363(8)
C(21)-C(22)	1.366(9)
C(22)-C(23)	1.383(6)

O(1)-Se(1)-C(17)	99.75(10)
O(1)-Se(1)-C(18)	103.43(12)
C(17)-Se(1)-C(18)	96.72(10)
C(16)-S(1)-C(17)	90.23(12)
F(2)-B(1)-F(1)	109.0(2)
F(2)-B(1)-N(1)	110.7(3)
F(1)-B(1)-N(1)	109.8(3)
F(2)-B(1)-N(2)	110.7(3)
F(1)-B(1)-N(2)	109.7(3)
N(1)-B(1)-N(2)	107.0(2)
C(2)-N(1)-C(6)	107.8(3)
C(2)-N(1)-B(1)	127.5(3)
C(6)-N(1)-B(1)	124.5(3)
C(8)-N(2)-C(12)	107.5(3)
C(8)-N(2)-B(1)	126.9(3)
C(12)-N(2)-B(1)	125.2(3)
N(1)-C(2)-C(3)	109.4(3)
N(1)-C(2)-C(1)	122.8(4)
C(3)-C(2)-C(1)	127.8(4)
C(4)-C(3)-C(2)	108.9(3)
C(3)-C(4)-C(6)	106.1(3)
C(3)-C(4)-C(5)	124.2(3)
C(6)-C(4)-C(5)	129.7(3)
C(13)-C(6)-N(1)	120.0(3)
C(13)-C(6)-C(4)	132.0(2)
N(1)-C(6)-C(4)	107.9(2)
N(2)-C(8)-C(9)	109.7(3)
N(2)-C(8)-C(7)	122.8(4)
C(9)-C(8)-C(7)	127.5(4)
C(10)-C(9)-C(8)	109.2(3)
C(9)-C(10)-C(12)	105.3(3)
C(9)-C(10)-C(11)	124.9(3)
C(12)-C(10)-C(11)	129.8(3)
C(13)-C(12)-N(2)	119.3(3)
C(13)-C(12)-C(10)	132.4(3)
N(2)-C(12)-C(10)	108.3(2)
C(12)-C(13)-C(6)	122.3(2)
C(12)-C(13)-C(14)	118.9(2)
C(6)-C(13)-C(14)	118.8(2)

C(17)-C(14)-C(15)	112.4(2)
C(17)-C(14)-C(13)	123.0(2)
C(15)-C(14)-C(13)	124.7(2)
C(16)-C(15)-C(14)	111.3(2)
C(15)-C(16)-S(1)	113.6(2)
C(15)-C(16)-Br(1)	126.7(2)
S(1)-C(16)-Br(1)	119.60(14)
C(14)-C(17)-S(1)	112.48(18)
C(14)-C(17)-Se(1)	130.67(18)
S(1)-C(17)-Se(1)	116.79(12)
C(23)-C(18)-C(19)	122.4(3)
C(23)-C(18)-Se(1)	119.6(3)
C(19)-C(18)-Se(1)	117.9(2)
C(18)-C(19)-C(20)	118.7(4)
C(21)-C(20)-C(19)	119.7(5)
C(20)-C(21)-C(22)	120.7(4)
C(21)-C(22)-C(23)	121.0(5)
C(18)-C(23)-C(22)	117.4(5)

Symmetry transformations used to generate equivalent atoms:

Table S3. Absorption energies with largest oscillator strength for **3**, **optimized 4** (B3LYP/6-31g* basis set and 6-311g* for Se and Br, G09) and **4** (from crystallography, non-optimized).

	f	Composition	CI (%)
3	0.2996	HOMO-2 → LUMO	3.36
		HOMO-1 → LUMO	19.7
		HOMO → LUMO	**77.7**
	0.1007	HOMO-2 → LUMO	2.74
		HOMO-1 → LUMO	**79.2**
		HOMO → LUMO	17.6
4	0.6524	HOMO-2 → LUMO	8.76
		HOMO-1 → LUMO	4.36
		HOMO → LUMO	**87.6**
Optimized **4**	0.3603	HOMO-2 → LUMO	2.46
		HOMO-1 → LUMO	2.63
		HOMO → LUMO	**93.7**
		HOMO → LUMO+1	2.24
Optimized **4'**	0.4053	HOMO-2 → LUMO	4.49
		HOMO → LUMO	**95.3**
		LUMO → HOMO	2.97

- END -